Biomaterials 175 (2018) 1–18

Contents lists available at ScienceDirect

Biomaterials

journal homepage: www.elsevier.com/locate/biomaterials

Decellularized and matured esophageal scaffold for circumferential esophagus replacement: Proof of concept in a pig model

Guillaume Luc [a, b, c, d], Guillaume Charles [a, b], Caroline Gronnier [b, d], Magali Cabau [a, b, d], Charlotte Kalisky [a, b], Mallory Meulle [a, b], Reine Bareille [b, c], Samantha Roques [a, b], Lionel Couraud [a, b, e], Johanna Rannou [a, b], Laurence Bordenave [a, b, c], Denis Collet [d], Marlène Durand [a, b, c, *]

[a] CHU Bordeaux, CIC1401, F-33000, Bordeaux, France
[b] Univ. Bordeaux, F-33000, Bordeaux, France
[c] Inserm, Bioingénierie tissulaire, U1026, F-33000, Bordeaux, France
[d] CHU Bordeaux, Department of Digestive Surgery, F-33000, Bordeaux, France
[e] LAPVSO, F-31201, Toulouse Cedex 2, France

ARTICLE INFO

Article history:
Received 14 March 2018
Received in revised form
9 May 2018
Accepted 14 May 2018
Available online 17 May 2018

Keywords:
Decellularization
Maturation
Esophageal scaffold
Pig implantation

ABSTRACT

Surgical resection of the esophagus requires sacrificing a long portion of it. Its replacement by the demanding gastric pull-up or colonic interposition techniques may be avoided by using short biologic scaffolds composed of decellularized matrix (DM). The aim of this study was to prepare, characterize, and assess the *in vivo* remodeling of DM and its clinical impact in a preclinical model. A dynamic chemical and enzymatic decellularization protocol of porcine esophagus was set up and optimized. The resulting DM was mechanically and biologically characterized by DNA quantification, histology, and histomorphometry techniques. Then, *in vitro* and *in vivo* tests were performed, such as DM recellularization with human or porcine adipose-derived stem cells, or porcine stromal vascular fraction, and maturation in rat omentum. Finally, the DM, matured or not, was implanted as a 5-cm-long esophagus substitute in an esophagectomized pig model. The developed protocol for esophageal DM fulfilled previously established criteria of decellularization and resulted in a scaffold that maintained important biologic components and an ultrastructure consistent with a basement membrane complex. *In vivo* implantation was compatible with life without major clinical complications. The DM's scaffold *in vitro* characteristics and *in vivo* implantation showed a pattern of constructive remodeling mimicking major native esophageal characteristics.

1. Introduction

Despite recent advances in esophageal surgery, the morbidity of esophagectomy remains high, with estimated postoperative complications ranging 30–60% [1–5]. The continuity of the post-esophagectomy gastrointestinal tract is preferably restored using gastric pull-up and sometimes the autologous interposition of other organs of the intestinal tract [6]. However, converting the stomach into an esophageal substitute is associated with deleterious changes, i.e., reduced gastric capacity, altered innervation, and damaged antireflux barrier [7]. In contradistinction to other tubular tissues such as the small intestine, lesion(s) of the esophagus require(s) ablating most of this organ for anatomical and oncological reasons, yet its lack of elasticity would preclude a tensionless anastomosis. Therefore, the need has arisen to develop segmental esophageal replacement techniques [8,9].

Esophageal tissue engineering is a promising approach to create an esophageal substitute [10] and improve clinical results in esophageal surgery. Various non-degradable and degradable esophageal scaffolds have been developed in tissue engineering. Luc et al. [10] described the pros and cons of 1) non-absorbable scaffolds, 2) polymeric absorbable scaffolds, and 3) decellularized

* Corresponding author. CIC-IT, PTIB/Hôpital Xavier Arnozan, Avenue du Haut Lévêque, 33600, Pessac, France.
E-mail address: Marlene.durand@chu-bordeaux.fr (M. Durand).

https://doi.org/10.1016/j.biomaterials.2018.05.023
0142-9612/

matrices (DMs) designed for this purpose. Non-absorbable scaffolds require stenting, leading to stenosis after stent removal and lack of tissue regeneration in large defects. Polymeric absorbale scaffolds release toxic degradation products, while the degradation rate is not controlled and the resulting structure is very different from the native tissue. DMs have the advantage of mimicking the native tissue and respect the architectural environment. Biological scaffolds composed of extracellular matrix (ECM) derived from decellularized tissue are increasingly used in regenerative medicine [11,12]. If tissue specificity is not essential in all tissue engineering applications [13], site-specific ECM preferentially maintains tissue-specific cell phenotypes, promote cell proliferation, and induce tissue-specific differentiation [14]. Decellularization is used to reduce inflammation and immunogenicity in an organ by removing its cellular elements and thus minimizing the functionality of the major histocompatibility complex (MHC), the root of self-recognition [15], while retaining the organ's mechanical and bioactive properties [6,16]. Beckstead et al. [2005] demonstrated that a decellularized human dermis (Alloderm©) offered a more favorable architecture to the organization of the epithelium when compared to cell-seeded polymeric scaffolds [17]. DMs contain the same components as ECM, i.e., glycoproteins, proteins, glycosaminoglycans (GAGs), and proteoglycans. These matrices mimic the biological and mechanical functions of native ECM and have a three-dimensional architecture associated with a microenvironment conducive to growth, proliferation, and cell orientation [6,16]. DMs are already used in vascular, cardiovascular, cutaneous, pulmonary, and urological applications and transpire as good candidates for esophageal tissue engineering. In previous experiments DMs were derived from stomach [8], bladder [18], and intestinal submucosa [8,18–20]. The use of DM allows reepithelialization [16,21], neo-angiogenesis [21], and muscle tissue obtention [16].

The aims of our study were to: (i) validate a standardized and reproducible model of decellularized esophagus, (ii) evaluate its histological composition and biomechanical behavior, (iii) evaluate possibilities of recellularization, and (iv) to evaluate its clinical relevance in a pig model.

2. Materials and methods

The various *in vitro* and *in vivo* experiments are summarized in Table 1. The procedures and handling of animals were based on the principles of Laboratory Animal Care formulated by the French National Society for Health and Medical Research, pursuant to European Directive #2010/63/EU and approved by the Animal Care and Experiment Committees. All experiments were carried out in accredited animal facilities.

2.1. Harvest and preparation of DM from porcine esophagus

The two lower thirds of esophagi were harvested from male pigs (45–55 kg) that had previously been involved in other experiments at the research facilities of Bordeaux University, i.e., DETERCA and IHU LIRYC (Bordeaux, France), pursuant to the recommendations of European Directive #2010/63/EU to reduce the number of animals to be used. With mechanical tests in mind, the pigs were specially purchased from supplying facilities accredited by Bordeaux University aiming to obtain sex, age, and weight homogeneity in a short period of time. Following euthanasia by an intravenous pentobarbiturate overdose (150 mg/kg), *post-mortem* esophagectomies were performed via thoracotomy by an experienced surgeon (G.L.). The esophagus adventitia was gently abraded. All samples were cut to an approximate length of 12 cm and preserved in a solution of Dulbecco's phosphate buffered saline (DPBS) (Gibco, Life Technologies, UK) containing 1% penicillin-streptomycin-amphotericin (PSA) at 4 °C until decellularization. In accordance with regulations, given that animals were directly euthanized without any other manipulation, no Ethics Committee approval was required.

2.1.1. Decellularization and assessment of DNA content

Esophagi were washed in DPBS (Gibco, Life Technologies), cannulated at both ends so as to be placed in a Bose Biodynamic Test® bench. The organs were fixed to the cannulas using 2-0 Vicryl ligatures (Ethicon) and infused with a peristaltic pump set to 70 mL/

Table 1
In vitro and *in vivo* experiments.

Study type		Material origin					Implanted animals		
		Pig				Human	Wistar rat	Nude rat	Pig
		NE	DM	pADSC	SVF	hADSC			
In vitro	Biological characterization	✓	✓						
	Mechanical characterization	✓	✓						
	Biocompatibility	-	✓			✓			
	Recellularization		✓	✓	-	-			
			✓	-	✓	-			
			✓	-	-	✓			
In vivo	Biocompatibility	✓	-				✓	-	
		-	✓				✓	-	
	Maturation without prior recellularization		✓				-	✓	
	Recellularization + maturation		✓	-	-	✓	-	✓	
	Model proof of concept	-	✓	-	-	-			✓

NE - native esophagus; DM - decellularized matrix; ADSC - adipose-derived stem cells.
The grey boxes represent non-applicable or nonsensical associations / tests; ✓ marks implemented associations / tests in the same experiment, - marks non-implemented association / tests in the same experiment.

min. The infusion protocol consisted of (i) a 12-hour cycle of water purified by reverse osmosis (resistivity 15 MegaOhm cm-1) with 0.9% w/v sodium azide (99.9%, Sigma-Aldrich), (ii) 24 h with 4% w/w sodium deoxycholate (Sigma-Aldrich) + 0.09% sodium azide w/v, and (iii) 12 h with 2000 Kunitz units of DNase-I (Sigma-Aldrich). Between cycles organs were rinsed for 6 h using PBS. All steps were carried out at room temperature with a reagent volume of 400 mL. After decellularization, each DM was stored in PBS and sterilized with gamma radiation at 25 kGy (Gammacell 3000 Elan MDS, Nordion).

DNA isolation and quantification were performed on native esophagi (NE) and DM (Supplementary material).

2.1.2. Biological characterization and biomechanical testing

Histology, immunohistochemistry analyses, and scanning electron microscopy (SEM) were performed and the concentration of sulfated glycosaminoglycans (sGAGs) determined in NE and DM (Supplementary material).

Longitudinal and circumferential mechanical tests were carried out by Rescoll® (France) with a Frame2 MTS 858 tabletop test system in physiologic solution (6 L, 48 g NaCl/1.2 g KCl/6.9 g Na_2H-$PO_4.2H_2O$/1.2 g KH_2PO_4) at 37 °C. Twenty-eight esophagi were tested as follows: longitudinal traction test on 7 NEs and 7 DMs and circumferential traction test on 7 NEs and 7 DMs. Strain (%), stress (kPa), elastic modulus (kPa), and strength (N) were measured in each sample. Burst tests were performed on a BOSE Biodynamic Test© bench at CIC-IT (Bordeaux, France). Twelve additional esophagi were tested: 6 NE and 6 DM in a physiological medium in a solution of Dulbecco's phosphate buffer saline (DPBS) 1X at 37 °C. Diameter variations were measured by a Mitutoyo® LSM 5035 micrometric laser scanner.

2.2. Biocompatibility

2.2.1. In vitro cytocompatibility

The DMs used for *in vitro* cytocompatibility studies had a last wash with Dulbecco's modified Eagle's medium DMEM/Ham's F-12 nutrient mixture 1:1 before irradiation.

2.2.1.1. Adipose tissue-derived stem cells (ADSCs) isolation and culture. Human ADSCs (hADSCs) were obtained from surgery waste of the Bordeaux University Hospital patients, in accordance with the provisions of law L. 1245-2 of the French Public Health regulation. hADSCs were isolated from human adipose tissue according to the technique of Bunnell et al. [22] with some modifications (detailed in the Supplementary material).

Pig ADSCs (pADSCs) were extracted from the retro-mandibular adipose tissue of the same animal whose esophagus was harvested (described above). The samples were collected under sterile conditions and stored in PBS with 1% PSA at 4 °C for a maximum of 48 h. The specimens were cut and prepared like the human adipose samples except that the cell pellet was taken up in erythrocytes lysis buffer (ELB) for 5 min with mechanical stirring and, after filtration at 100 μm, the whole was centrifuged at 1200 rpm for 10 min. Then, 1% PSA and 50 μg/mL of gentamicin were added to DMEM/Ham's F-12 1:1. The obtained porcine stromal vascular fraction (SVF) was either directly cryopreserved or cultured in suitable culture flasks, treated to promote adhesion and cell growth and to isolate the pADSCs. The flasks were placed in an incubator at 37 °C, 5% CO_2, and 85% humidity.

2.2.1.2. Cytotoxicity tests. Two techniques were used to evaluate the cytotoxicity of released products generated by decellularization and/or sterilization: the MTT test (3-(4-5-dimethylthiasol-2-yl) diphenyl tetrazolium bromide) to quantify metabolic activity [23] and the neutral red (NR) assay to evaluate hADSC cell viability [24] (Supplementary material).

2.2.1.3. hADSC adhesion test. The adhesion of hADSCs after seeding was tested over 3, 6, and 24 h under static conditions on plastic control and DM (Supplementary material).

2.2.2. In vivo biocompatibility

Adult non-immunosuppressed Wistar rats were subcutaneously implanted in order to study the biocompatibility of NEs and DMs in terms of host response. The procedures and handling of animals were approved by the Animal Care and Experiment Committee (CEEA50) of Bordeaux University, France (authorization #1363 of 12-Nov-2014) (Supplementary material). Semi-quantitative histomorphologic analysis was perfomed on the explanted tissue after sacrifice (Supplementary material).

2.3. Recellularization

2.3.1. In vitro recellularization assays

Various issues of DM recellularization were investigated: either *in vitro* or *in vivo*, with sheets or cell suspensions, by external or intraluminal seeding.

2.3.1.1. Internal/external seeding with hADSC sheet. hADSCs obtained after passage 2 were seeded at 10 000 cells/cm^2 in peelable T150 culture flasks. The used medium was composed of DMEM/Ham's F-12 3:1, 10% (v/v) SVF, 1% (v/v) antibiotic antimycotic solution (AAS containing penicillin 10 000 U/streptomycin 10 mg/amphotericin 25 μg (Sigma©, France), and 50 μg/mL ascorbic acid. The culture flasks were incubated in a humid atmosphere at 37 °C, 5% CO_2. The media were changed 3 times a week. A ballasting system was necessary to avoid the early detachment of sheets from flasks. Seeding of the outer surface was done by placing the DM onto the hADSC sheet, resulting in adherence between them. The DM was rolled up in the hADSC sheet over 2–3 convolutions. The method of seeding the inner surface was similar but required prior manual eversion of the DM. After 14 days in culture, it was reverted to the original state so as to seed the outer surface by placing the DM onto a new sheet. Once both sides were seeded, the DM/sheet complexes were maintained in T150 culture dishes associated with culture medium similar to hADSCs for 21 additional days. Analysis of the DM/sheet complexes was done by histology with HES staining on days D0, D14, D21, D28, and D35 after internal seeding. The hADSCs were characterized both before and after 30 days of sheet culture by flow cytometry, whereas their ability to express markers of adipocytes, chondrocytes, osteoblasts, and smooth muscle cells was assessed with or without differentiating media (Supplementary material).

2.3.1.2. Intraluminal seeding with pig cell suspensions. DMs were installed in a sterile Bose BioDynamic Test© bench between 2 connectors, and then seeded with a density of 250,000 cells/cm^2 of the internal esophageal wall. Seeding of the DMs was performed with either pADSCs or pSVF, injected with a syringe through the connectors, and 5 mL of DMEM/Ham's F-12 1:1 + 10% FCS + 1% AAS were injected approximately simultaneously through the connectors. Slight overpressure was applied for a few seconds to force cell passage through the different layers of the DM. Medium was then added to the chamber. The chamber was placed in the incubator at 37 °C, 5% CO_2, and 85% humidity for 4 h and 24 h. The medium contained in the lumen of the DM was renewed every day. After the desired incubation time, the DMs were placed in 4% formaldehyde for histological analysis and compared with the unseeded samples.

2.3.2. In vivo omental maturation

To assess the biological efficiency of *in vivo* recellularization process by omental maturation, 8-week-old nude rats (male, 270–330 g) (Charles River Laboratories, France) were operated via median laparotomy under general anesthesia. The procedures and handling of rats were approved by the Animal Care and Experiment Committee (CEEA50) of Bordeaux University, France (authorization #DIR1369, 17-Mar-2015). Implantation of the DM in rats' omentum was performed in 30 animals divided in 3 groups of 10, followed up for 2, 4, and 8 weeks, respectively. Two conditions were tested: DM versus DM cellularized with a sheet of hADSC (cDM). In each group 5 rats received a 1-cm^2 sample of DM or cDM, rolled up in omentum and fixed with interrupted stiches using 4/0 non-resorbable sutures. The abdominal wall was closed in the usual manner. Rats were euthanized 2, 4 or 8 weeks after implantation in order to evaluate the optimal maturation time, i.e., the effect of time and DM cellularization on inflammation and vascularization. Each sample was placed in 4% formaldehyde and histological analyses were performed after hematoxylin-eosin-saffron (HES) staining.

2.4. Proof of concept: feasibility of the DM transplantation with or without previous maturation, in a pig model of esophagus substitution

The aim of this experimental protocol was to evaluate the feasibility of esophageal replacement by DM after prior omental maturation or without it. The procedures and handling of pigs were approved by the Animal Care and Experiment Committee of INRA 084, France (authorization #2015101211046416 of 24-Feb-2017). Twelve male 10-12-week-old domestic pigs with weights ranging 37–47 kg were used (6 donors for DM production and 6 recipients). The recipient animals were accustomed to a liquid diet for two weeks and then fasted 24 h pre-operatively. They underwent standard endotracheal general anesthesia after induction. The animals were positioned in the dorsal decubitus position.

Recipient pigs were randomized in 2 groups: receiving DM after maturation in their own omentum (n = 3) versus DM without prior omental maturation (n = 3). In the former group midline laparotomy led to exposure of the greater omentum. An 8-cm-long DM was stented by 20-Fr Foley catheter and rolled up in omentum (Fig. 1 A). The muscle-aponeurotic layer and skin were closed in the usual manner. The DM was removed 4 weeks later (Fig. 1B and C) and transposed in the same animal.

Median laparotomy was performed for DM implantation (n = 6), i.e., transposition from omentum (n = 3) and *de novo* implantation (n = 3). The abdominal esophagus was transected and resected to generate a 5-cm-long, full-thickness circumferential defect. The gastroesophageal junction was left out of the resected defect in order to suture the DM to the esophagus and not the stomach. DM was placed in the esophageal defect and sutured to the esophageal edges by interrupted 4/0 PDS (polydioxanone) end-to-end stiches. In the maturation group, DM was transposed respecting omental vascularization. In the non-maturation group, a cover omentoplasty was performed around the DM and the anastomoses. The abdominal wall was closed by running sutures. Stent and abdominal/thoracic drains were not left *in situ*. The post-operative care protocol is described in the Supplementary material. After 5 weeks, all pigs were sacrificed; the DMs and adjacent tissues were harvested and underwent histochemistry analysis under Masson's trichrome staining.

2.5. Statistical analysis

Quantitative data are reported as mean ± standard deviation. The distribution of the samples was considered Normal. The independent continuous variables were compared by the Student's test. Comparison of two percentages (categorical variables) was made by the Chi-square test or Fisher's exact test, whichever appropriate. Comparison of means of continuous variables was made by means of Student's t-test. The cut-off for statistical significance was set at $p \leq 5\%$. The data analysis was performed on the SPSS software, version 11.0 (Statistical Package for the Social Sciences, Chicago, IL, USA).

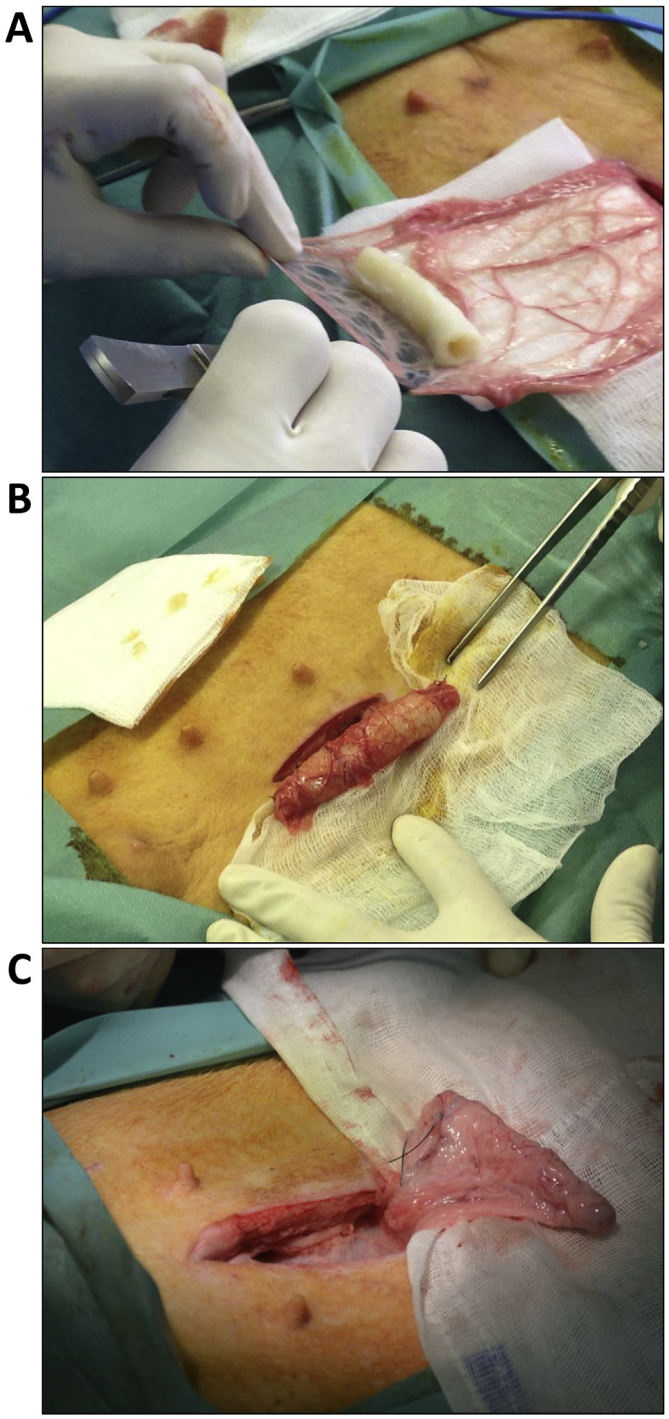

Fig. 1. Surgery Surgical view of DM implantation in the porcine omentum (A), 4 weeks after maturation before transposition (B, C).

3. Results

3.1. Harvest and preparation of DM from porcine esophagus

A total of 186 eight-week-old pigs, either female or male, were used in the study to prepare and characterize esophageal scaffolds, of which 101 were used for the development of the decellularization process, 40 for the mechanical tests, 33 for the cellularization experiments, and 12 for *in vivo* studies.

3.1.1. Decellularization and assessment of DNA content

The macroscopic aspect changed during the decellularization process: DM turned translucent and thicker than the native esophagi (NE) (Fig. 2, A, a and b). Decellularization fulfilled the pertinent criteria [25], i.e., no intact nuclei were visible by HES staining (Fig. 2, B, b), the concentration of remnant DNA in DM (50 ± 18 ng/mg) was markedly less than that in NE tissue (1630 ± 141 ng/mg) ($p < 0.001$) (Fig. 2, C), and residual DNA was present only in fragments less than 200 bp in length (Fig. 2, D).

3.1.2. Biological characterization and biomechanical testing

The concentration of sGAGs was lower in DM than in NE: 0.19 ± 0.02 μg/mg vs. 0.27 ± 0.03 μg/mg of dry tissue, respectively ($p > 0.0001$) (Fig. 3, A). Alcian blue staining demonstrated sGAGs in

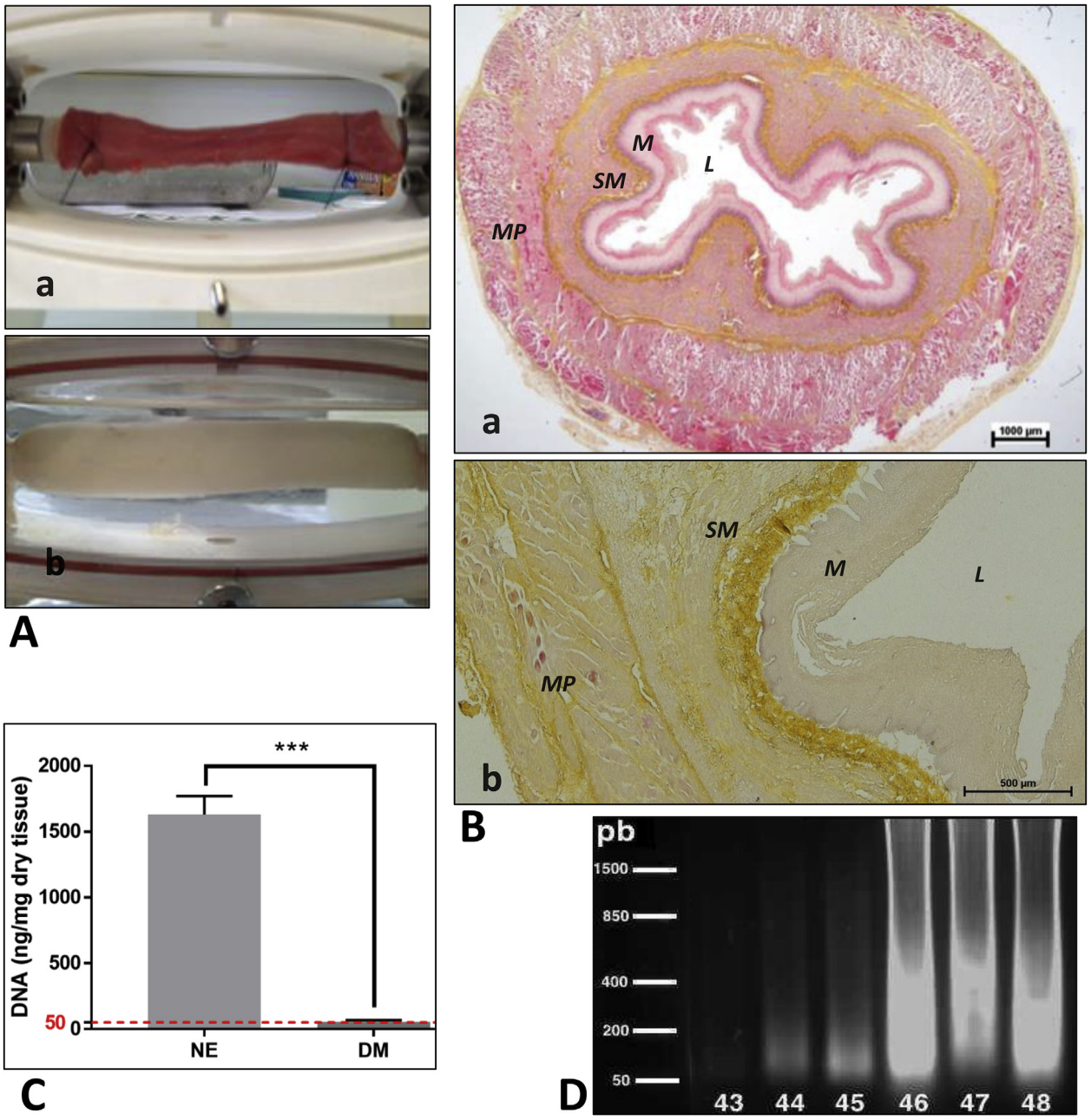

Fig. 2. Assessment of esophageal decellularization, A. Macroscopic aspect of porcine esophagus before (a) and after (b) decellularization, B. Hematoxylin, eosin and saffron (HES) staining histomicrographs before (a, x10) and after (b, x100) decellularization. No intact nuclei were visible after decellularization, while the ultrastructure was preserved (b). L – lumen; M – mucosa; SM – submucosa; MP – muscularis propria, C. The concentration of remnant DNA in DM extraction was 1630 ng/mg of native esophagus (NE) tissue dry weight versus 50 ng/mg of DM dry weight. *** $p < 0.001$, D: Residual DNA was present in DM with fragments shorter than 200 bp (43, 44, and 45). Residual DNA was present in NE in fragments longer than 200 bp (46, 47, and 48).

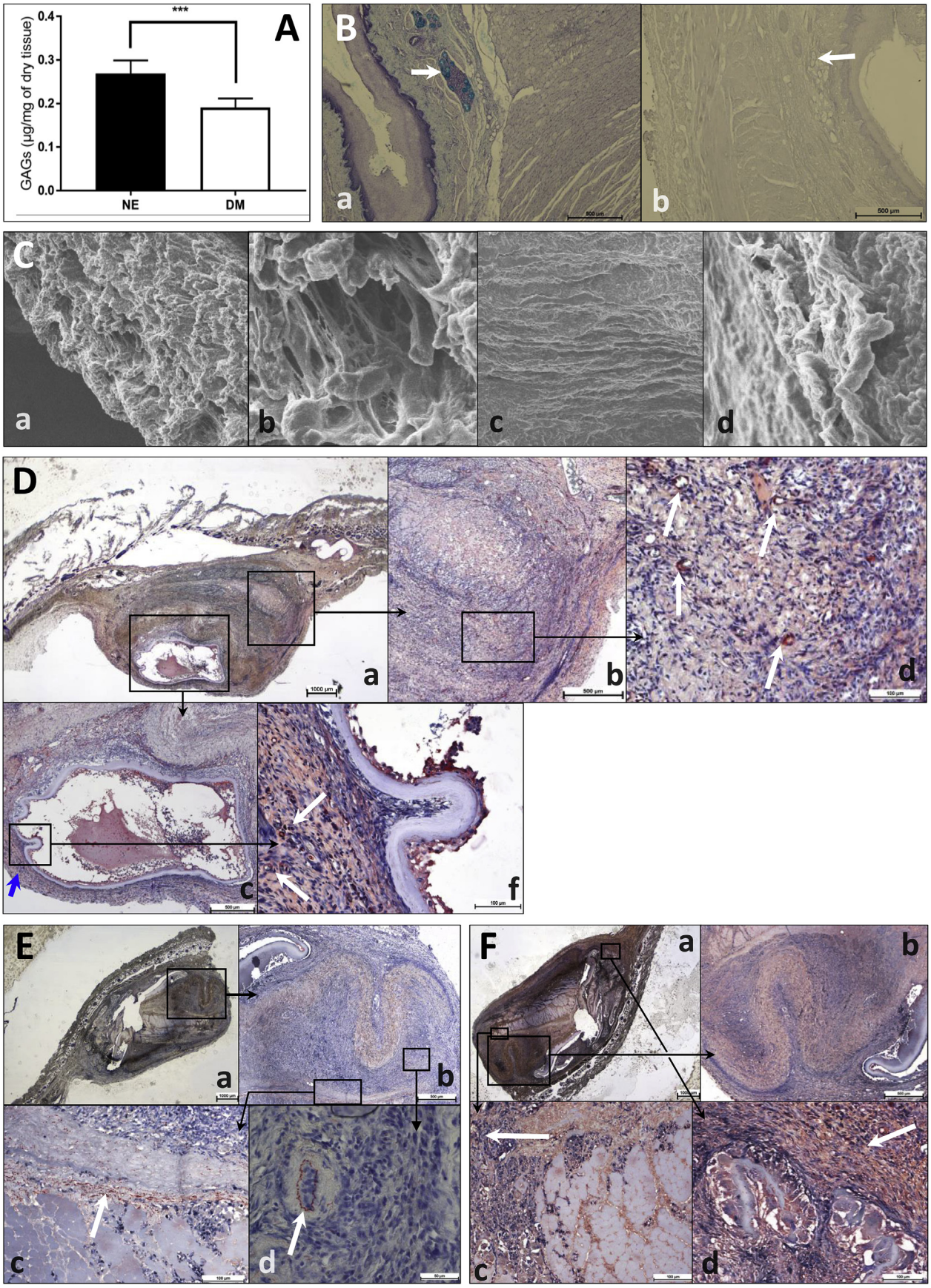

Fig. 3. Structure, A. Concentration of sulfated glycosaminoglycans (sGAGs) before (NE) and after decellularization (DM) in dry weight tissue. The concentration decreased significantly after decellularization. *** ($p < 0.0001$), B. Alcian blue staining histomicrographs (x40) showing more GAGs in glands of NE (a, white arrow) than in DM samples (b,

the NE submucosa and to a lesser degree after decellularization (Fig. 3, B).

SEM images of the luminal and external surfaces disclosed that DM had a smoother luminal surface, in contrast with the external surface that had a more textured and fibrous structure (Fig. 3, C).

The spatial distribution of ECM proteins (laminin, elastin and fibronectin) was preserved after decellularization, as revealed by immunohistochemistry analysis (Fig. 3, D, C, F).

The biaxial stress response of NE showed an anisotropic behavior, i.e., a maximum strain of 104% and 95% in the circumferential and longitudinal directions, respectively. DM showed similar anisotropy, with a maximum strain of 65% and 387% in the circumferential and longitudinal directions, respectively. Table 2 details the results of biomechanical tests. Compared to NE, DM demonstrated (i) a significant strain reduction in the longitudinal axis and significant strain increase in the circumferential direction, (ii) a significant increase of stress in the longitudinal axis but no significant change in the circumferential direction, (iii) an important and significant rise of elastic modulus in the longitudinal axis and its significant decrease in the circumferential axis, and (iv) a significant increase in the longitudinal axis strength but no significant change in the circumferential direction.

Burst pressure could not be reached with DM, whereas it marked 79.2 kPa ± 20.9 for NE. The porosity resulting from the decellularization process induced a liquid leakage through the DM wall (Fig. 4, B). The maximal pressure reached with DM was 108.3 kPa ± 17.9, with constant leakage through the wall at that pressure. No significant difference was observed between the two groups in terms of endoluminal pressure ($p = 0.386$).

3.2. Biocompatibility

3.2.1. In vitro cytocompatibility

3.2.1.1. Cytotoxicity testing. The neutral red assay exhibited mean cellular viability rates of 89% ± 21 at 24 h, 103% ± 6 at 48 h, and 100% ± 5 at 72 h for DM when compared to control. The MTT test found mean metabolic activity/viable cells of 81% ± 22 at 24 h, 95% ± 9 at 48 h, and 91% ± 11 at 72 h for DM when compared to control. The increase of hADSC viability and metabolic activity with immersion time was statistically significant ($p < 0.0001$) in all conditions, except for positive control (Triton x-100). Assuming a 70% toxicity limit [23], it can be stated that DM displayed a non-cytotoxic profile in both tests (Fig. 5, A).

3.2.1.2. hADSCs adhesion test. The attachment of hADSCs on DM was observed thanks to Td-tomato labelling confirming that hADSCs were present after 10 days of *in vitro* culture (Fig. 5, B). The rates of hADSCs adhesion to DM were 40% ± 13, 43% ± 13, and 49% ± 12 at 3 h, 6 h, and 24 h, respectively. The increase of hADSC adhesion with testing time was statistically significant ($p < 0.0001$) for all conditions.

3.2.2. In vivo biocompatibility

All specimens were alive at the end point. The Wistar rats had an uneventful post-implantation period. Encapsulation of the DM was not detected (Fig. 5, C, a). The *in vivo* host reaction to DM scaffold after 14 and 35 days consisted in an inflammatory cell response, mainly of mononuclear cells (Fig. 5, C, b, c, and d). Performed accordingly to the protocol detailed in Supplementary data, a semi-quantitative histomorphologic analysis at day 14 and day 35 yielded histologic scores of 12.3 ± 1 and 8 ± 2, respectively.

3.3. Recellularization with hADSC, pADSC, and pSVF

3.3.1. In vitro recellularization assays

3.3.1.1. Internal/external seeding with hADSC sheets. The extracted hADSCs were able to differentiate into osteoblasts, chondrocytes, adipocytes, or smooth muscle cells [Fig. 6A and B, C, D]. After 30 days of sheet culture, they kept their ADSC flow cytometry profile ($CD31^{-}$, $CD45^{-}$, and $HLA\text{-}DR^{-}$, with 80–100% of cells being $CD73^{+}$, $CD90^{+}$, $CD105^{+}$); they also showed no positive staining with Oil red, Alcian blue, Alizarin red, and actine/myosine heavy-chain, similarly to the control hADSCs [Fig. 6E and F, G, H]. However, they stained positive for calponin and SM22, which was in contrast to control hADSC (Supplementary material).

Three DMs were seeded on the internal surface for 14 days and then seeded on the external surface for 21 additional days. Samples cut on day 0 (before seeding) confirmed the absence of nuclei within the DM. On samples cut on day 35 the hADSC sheet is observable and adheres to the residual adventitia (Fig. 7, A). At the level of the adhesion zones, the ADSCs seem to have migrated from the external surface to the muscularis confirmed by the presence of nuclei in violet. But ADSCs did not migrate from the sheet in the lumen to the underlying muscularis, except through a crack in the mucosa. Accordingly, we decided to remove this “natural barrier”, the epithelium of the mucosa, before the seeding experiments that follow.

3.3.1.2. Intraluminal seeding with pig cell suspensions. As soon as 4 h after seeding, pADSCs were found along the submucosa in the

Table 2
Mechanical characteristics of native esophagus and decellularized esophagus (extracellular matrix) in the circumferential and longitudinal directions.

Characteristic	Longitudinal			Circumferential		
	Mean ± SD		P^a	Mean ± SD		P^a
	NE (n = 7)	DE (n = 7)		NE (n = 7)	DE (n = 7)	
Strain (%)	95 ± 20	42 ± 11	<0.001	102 ± 16	366 ± 254	0.033
Stress (kPa)	280 ± 69	1384 ± 932	<0.001	160 ± 44	146 ± 32	0.548
Elastic modulus (kPa)	621 ± 149	5974 ± 2551	<0.001	279 ± 16	89 ± 53	<0.001
Strength (N)	33 ± 7	68 ± 13	<0.001	107 ± 25	93 ± 23	0.289

[a] Student's t-test. SD – standard deviation; NE – native esophagus; DE – decellularized esophagus.

white arrow), C. Scanning electron micrographs (SEM) of the DM's surfaces (x100). The external surface was more textured and fibrous (a,b), whereas the luminal surface was smoother (c,d), D. Anti-laminin Ab immunohistochemistry micrographs of a DM sample, showing the presence of laminin (a, x10). Namely, laminin was demonstrated in the submucosa (b, x40) and in muscularis layer (c, x40). At higher magnification laminin is seen in the submucosa (d, x200, white arrow) and muscularis (f, x200, white arrow), E. Anti-elastin Ab immunohistochemistry micrographs of the DM sample showing the presence of elastin (a, x10). Elastin was present in the muscularis layer (b, x40; c, x200, white arrow). Elastin was foremost demonstrated around capillaries in the submucosa (d, x400, white arrow), F. Anti-fibronectin Ab immunohistochemistry micrographs of the DM sample showing the presence of fibronectin (a, x10). Fibronectin was present in muscularis layer b (x40), c (x200, white arrow). At higher magnification fibronectin is shown in both submucosa and muscularis layer (d, x200, white arrow).

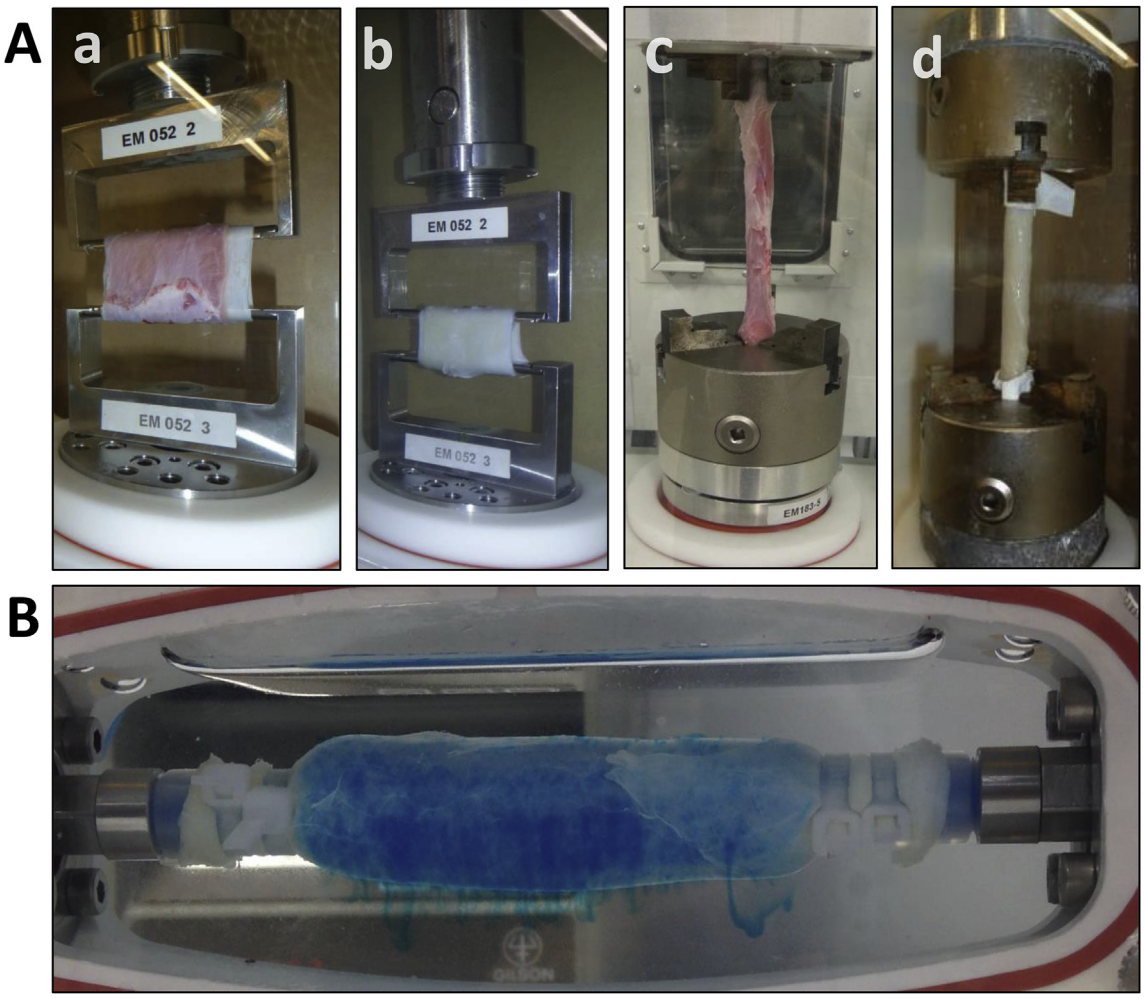

Fig. 4. Biomechanics, A. Mechanical characterization of NE and DM. Equipment with intact samples for circumferential (NE in a, DM in b) and longitudinal (NE in c, DM in d) traction tests, B. Burst pressure in DM sample with Patent Blue V exhibiting leakage through the walls of the DM.

form of clusters or aligned cells (Fig. 7, B, a); they coated the luminal surface in a continuous organized layer of brick-shaped cells and penetrated and remained sporadically viable in the submucosa (SM). These pADSCs in the SM are either spindle-shaped or round, i.e. their appearance and density are indeed different from the continuous layer on the surface. In counter distinction, four hours after seeding a DM with pSVF, cells were visible on or within the submucosa, sometimes up to the level of the muscularis. These cells were round and rather isolated from one another (Fig. 7, B, b). However, no other cells were found in the mid-section of the DM.

3.3.2. In vivo omental maturation

3.3.2.1. Implantation of DM, seeded with hADSC or not, in nude rats' omentum. The postoperative period was uneventful, with a satisfying postoperative weight gain (data not shown) demonstrating the tolerability of the procedure.

At 2 weeks post-op, DMs were intact and maintained histological organization, i.e., all three layers were present. The mean ± SD estimated cellularization was 111 ± 37 cells/10 fields in DM with prior ADSCs seeding, versus 99 ± 44 cells/10 fields in DM without ADSCs ($p > 0.1$). The presence of ADSCs did not modify vascularization (2 ± 0 for DM + ADSCs versus 2.5 ± 0.5 in DM without ADSCs ($p > 0.1$)).

At 4 weeks post-implantation, DMs were still present but the muscularis layer was partially degraded (Fig. 7, C, a, b). Cellularization was estimated at 65 ± 15 cells/10 fields in DM with previous ADSCs seeding, versus 60 cells ± 5/10 fields in the DM without ADSCs ($p > 0.1$). The presence of ADSCs did not modify vascularization (1.5 ± 1 in DM with ADSCs versus 1.75 ± 0.5 in DM without ADSCs ($p > 0.1$)).

At 8 weeks post-implantation DMs were entirely degraded, with the three histological no longer identifiable (not shown). Cellularization marked 55 ± 24 cells/10 fields in DM with previously ADSCs seeding, versus 44 ± 18 cells/10 fields in ECM without ADSCs ($p > 0.1$). The presence of ADSCs did not modify vascularization (2 ± 0 in DM + ADSCs versus 2.5 ± 0.5 in DM without ADSCs ($p > 0.1$)).

3.4. Proof of concept: feasibility of DM transplantation with or without previous maturation in a pig model of esophagus substitution

The graft was clinically well-tolerated globally and proved functional as witnessed by weight regain. Five of the six animals never reached class 3–4 critical endpoints during the entire follow-up. One specimen in the maturation group died of sepsis on the first postoperative day.

Macroscopic analysis showed that the 4-week matured DM was more fibrous and seemed less resilient according to the surgeon. Histological analysis showed cell infiltration (Fig. 8A and b & d)

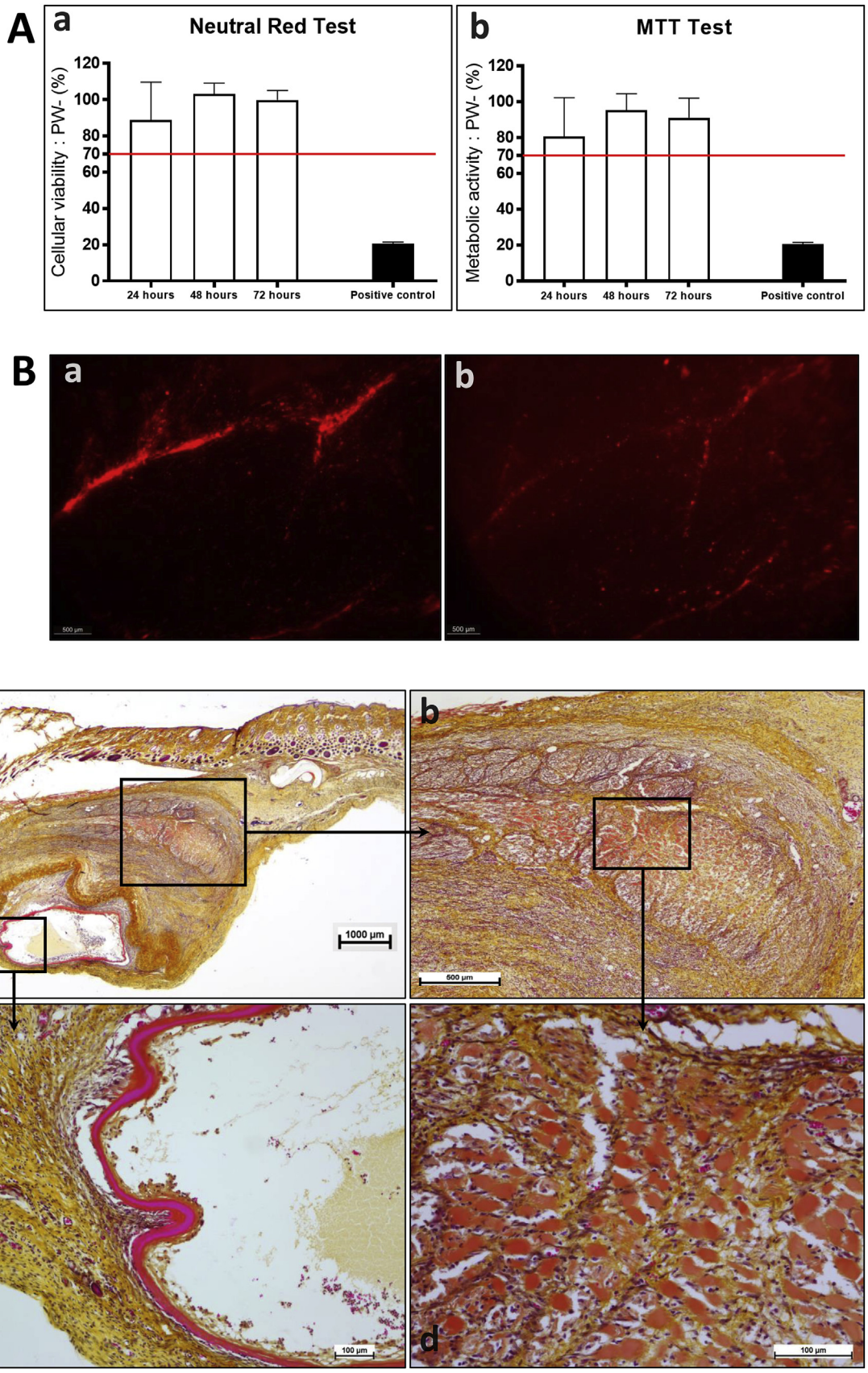

Fig. 5. Biocompatibility, A. Neutral red test and colorimetric MTT (3-(4,5-dimethylthiazol-2-yl)-2,5-diphenyl tetrazolium bromide) assay in the final rinsing water of the DM preparation. Cell viability and metabolic activity were higher than 70% at all incubation times, showing no DM cytotoxicity, whereas the positive control (Triton x-100) was below 70%, as expected, B. Fluorescence micrograph 24 h (a) and 10 days (b) after manual seeding of hADSCs Td-tomato on DM, showing the ability of hADSCs to adhere and survive on DM, C. Histomicrographs of a DM sample 14-day post-implantation in the abdominal wall of a Wistar rat under hematoxylin, eosin and saffron (HES) staining. Encapsulation of DM was not present (a, x10). There was inflammatory response with cells infiltrating the residual muscularis layer (b, x40) and degradation of the mucosa along with cell infiltration (c, x100). Mononuclear cells are visible at higher magnification in the muscularis layer (d, x200).

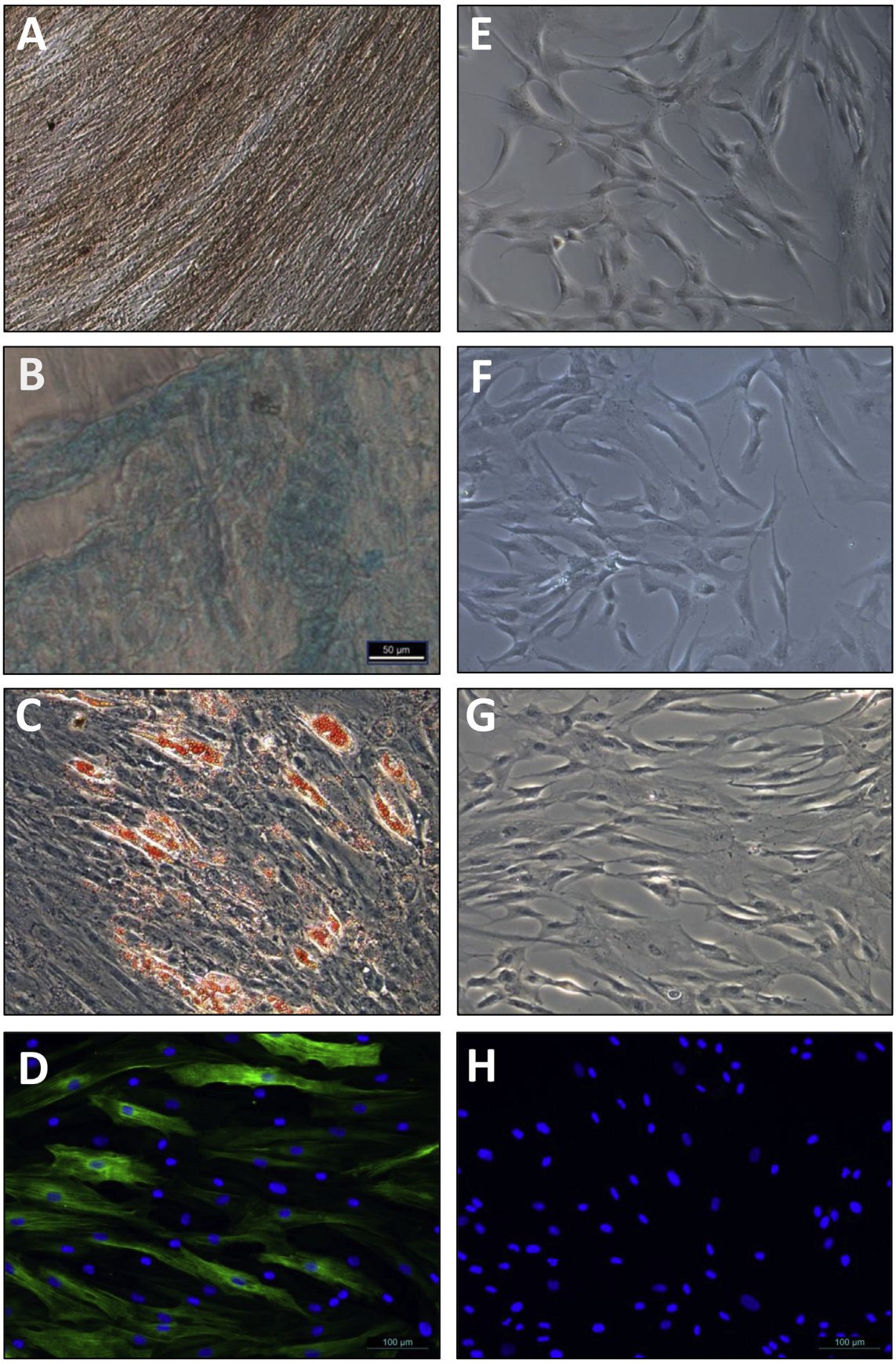

Fig. 6. hASC characterization, Images in the left column demonstrate that extracted hASCs show positive staining for markers of osteoblasts (A, Red alizarin), chondrocytes (B, Alcian blue), adipocytes (C, Oil red), and smooth muscle cells (D, anti-MHC immuno-staining) after culture in differentiation media. Images in the right column show the same extracted hASC but after 30-day culture in sheet showing no positive staining for the markers of those lineages (E – Red alizarin, F – Alcian blue, G – Oil red, and H – anti-MHC immunostaining) demonstrating the preservation of their hASCs phenotype.

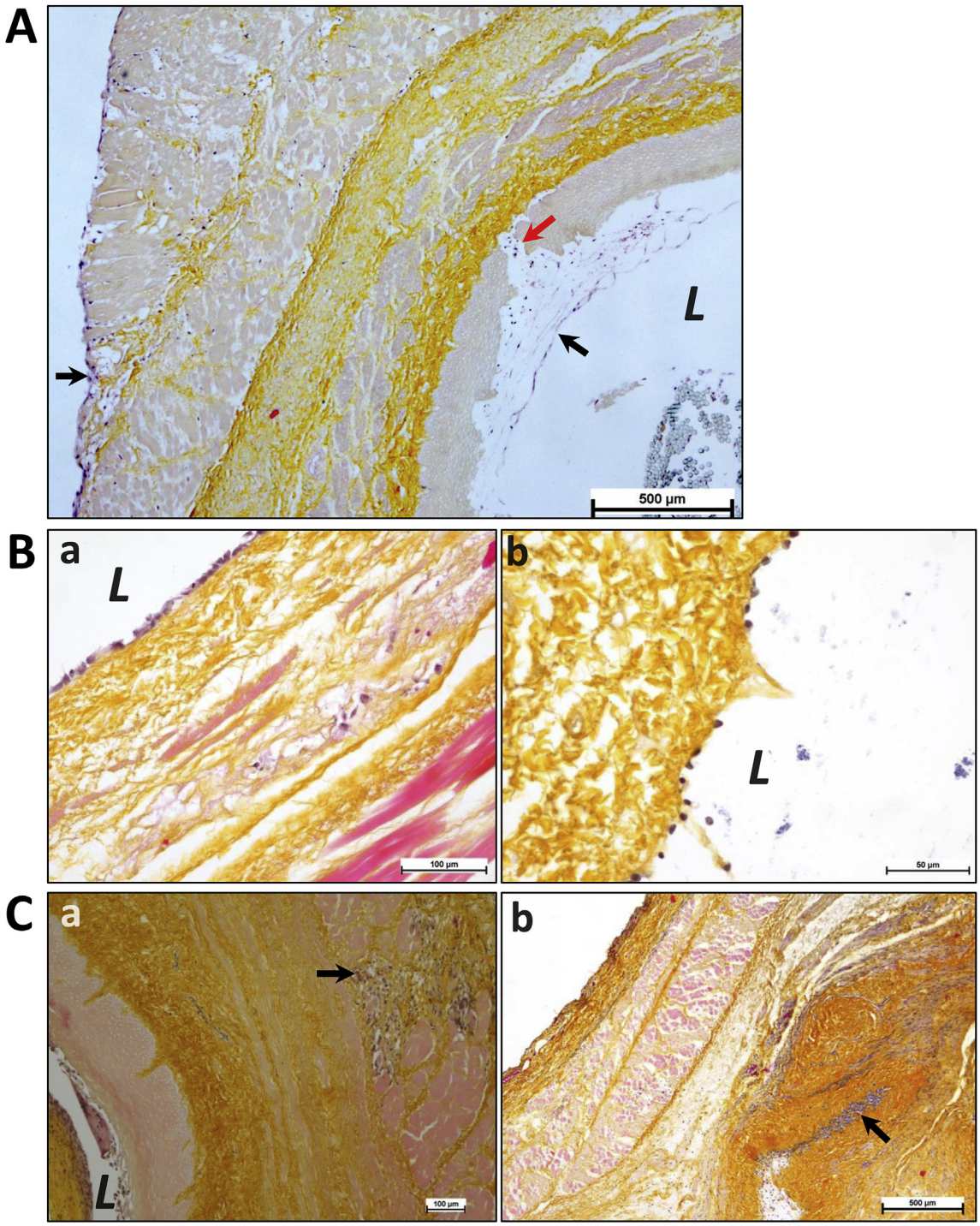

Fig. 7. Recellularization and seeding, A. Histomicrograph under hematoxylin eosin and saffron (HES) staining showing DM after 35 days of seeding with hADSCs sheets. The presence of cells on the external and internal surfaces is shown (black arrows pointing to layers of the ADSC sheet), along with the scarcity of intact nuclei in DM's submucosa and their total absence from the muscularis layer. At the level of the adhesion zones, the ADSCs seem to have migrated from the external surface to the muscularis externa (presence of some nuclei in violet). On the mucosal side migration of ADSCs did not occur from the lumen but an adhesion to the underlying muscularis mucosa was possible through a crack in the mucosa (red arrow) (a and b, x40). L – lumen, B. HES-staining histomicrographs of DMs after 4-hour intraluminal seeding with pADSC (a, x200) and pSVF (b, x400). Both histomicrographs reveal cells, although of different shapes: elongated and organized cells present along or within the submucosa after seeding with pADSC (a) versus round and isolated cells along the submucosa after seeding with pSVF (b). L – luminal side, C. HES-staining histomicrographs of DMs 4 weeks after implantation in nude rat omentum: DM without hADSCs sheet seeding (a, x100) and DM seeded with hADSCs sheet (b, x40). In both, cells were present in the DM (black arrows pointing to clusters of violet nuclei). (For interpretation of the references to color in this figure legend, the reader is referred to the Web version of this article.)

from the periphery to the center, more intense in the muscularis layer but also in the submucosa. Vascularization was mainly present in the muscle layer. A minor encapsulation was evidenced by the presence of fibroblasts and the DM's fibrous macroscopic aspect. Immunohistochemistry enhanced the presence of cells with alpha-actin expression, which may be muscular cells or

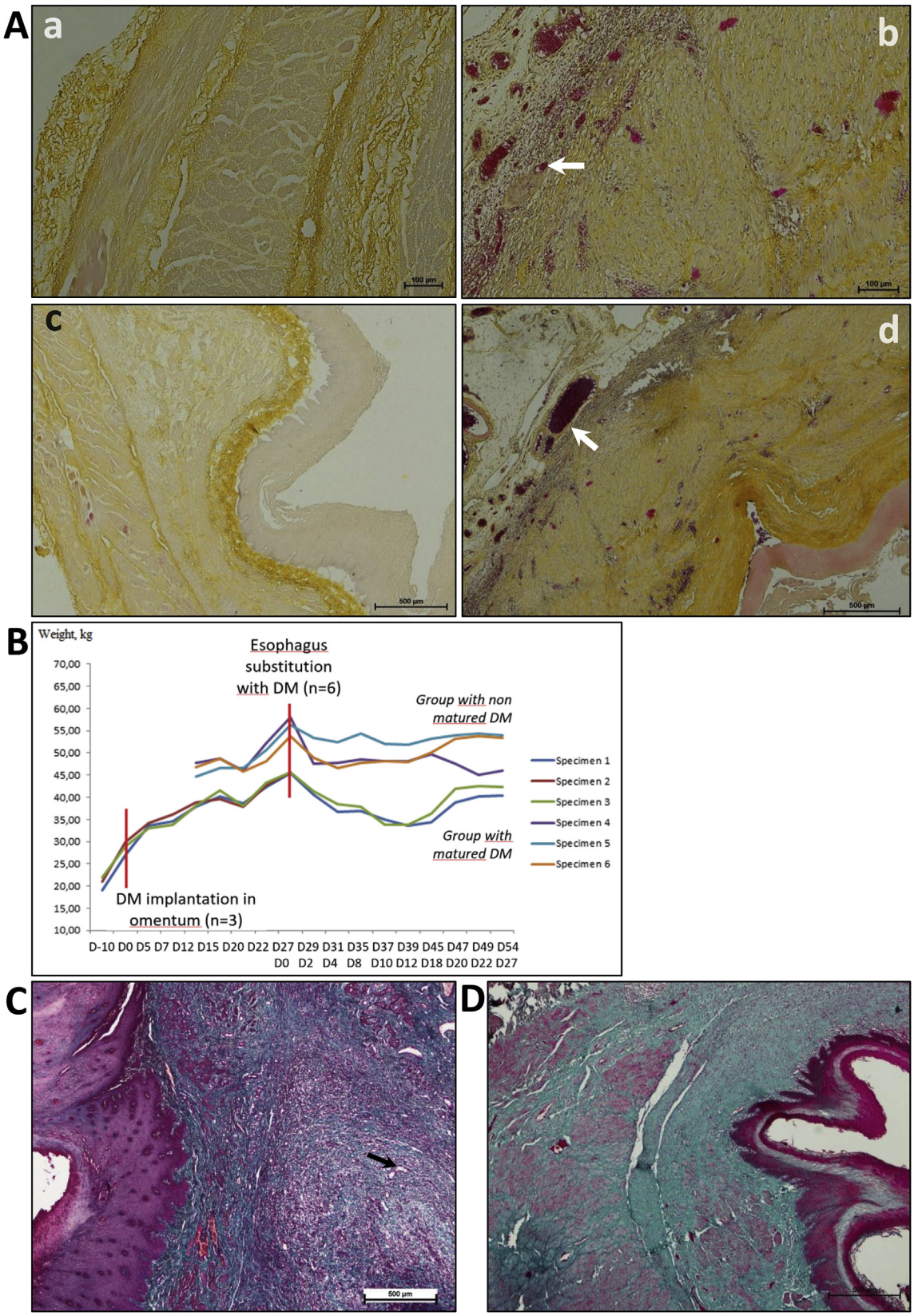

Fig. 8. Maturation and implantation, A. Histomicrograph under HES staining showing a DM before maturation with no intact nuclei in the DM and the three structural layers still present (a, x100; c, x40) and after four weeks of maturation in porcine omentum (b, x100; d, x40). The presence of cell infiltration and vascularization is marked by black arrow in b (x100). The junction between omentum and DM is pointed out with by a black arrow in d (x40). The presence of cell infiltration is visible throughout the DM, from periphery to center in b and d, B. Post-operative weight curves of the six pigs, C. Histomicrograph under Masson's trichrome staining showing DM 5 weeks after esophageal replacement in a pig with prior omentum maturation (x40) with its 3 structural layers. Inflammatory cells were present in the mucosa, with histologic organization and vascularization by capillaries (black arrow) mainly in the muscle layer. Muscle tissue was undergoing remodeling, D. Histomicrograph under Masson's trichrome staining of DM 5 weeks after esophageal replacement in a pig without prior omentum maturation (x10) with the 3 structural layers. Mononuclear cells were present in all three layers. The histological organization was not preserved and the connective tissue not organized.

myofibroblasts.

The DM was easily suturable during surgery and kept its integrity. The surviving five animals were alive at the end of the 5-week follow-up. Their weight decreased in the first week following implantation, then increased over the next 4 weeks (Fig. 8, B). All animals had postoperative complications with the exception of specimen 5; these pathologies were observed upon macroscopic inspection at explantation, i.e., 2 stenoses with esophageal dilatation, 3 abscesses (2 peri-anastomosis and 1 pleural), 2 proximal anastomosis leakages, and 1 pulmonary infection (Table 3). The mean weight loss was 17.4% ± 7.7, and 4 out of 5 pigs regained their preoperative weight after one month.

At histological analysis under Masson's trichrome staining, DM with previous maturation in omentum exhibited cellularization and vascularization near the proximal and distal anastomotic areas. The mucosa and submucosa were preserved with cells present, while fibrosis was in progress and vascularization seen in the muscularis layer (Fig. 8, C). Fibrotic tissue was mainly observed in mid-section of the DM (data not shown). In the proximal and distal perianastomotic zones of DM that had not undergone prior omental maturation, there was cellularization, with a preserved architectural structure of the mucosal and submucosal layers, while blood vessels were observed in the muscularis and submucosal layers. The connective tissue was not well organized. The muscular layer was not organized or entirely absent and infiltration by inflammatory cells was pronounced. Mononuclear cells were present in the all three histological layers. (Fig. 8, D).

4. Discussion

The aims of the present study were to (i) validate a standardized and reproducible model of decellularized esophagus, (ii) evaluate its histological composition and biomechanical behavior, (iii) evaluate its recellularization potential, and (iv) evaluate its clinical impact in a pig model of esophagectomy.

4.1. Harvesting

The homogeneity of pigs in terms of age and weight was a mandatory prerequisite in order to validate the decellularization process. The availability of appropriate animals sacrificed in previous experiments has been a significant issue all along the project: the authors' strategy to minimize the number of animals to be sacrificed solely for harvest greatly complicated the course of the study. Harvesting of esophagi and adipose tissue were performed in very strict surgical conditions to prevent bacterial contamination. The source of esophagi originating from animals submitted to previous protocols demonstrated to be feasible, cheap, ethical, and efficient.

4.2. Decellularization

Our findings assessed the good quality and reproducibility of decellularization according to previously established criteria [25]. Numerous methods of decellularization yielding random results have been described in the literature [10]. Our choice to use a dynamic detergent/enzymatic method was carried out to avoid using chemical agents criticized for their cytotoxic potential and also to preserve the structure of the ECM that allows cell migration, proliferation, and differentiation [14]. In addition, the influence of ECM has also been described in mitogenesis [26], cell differentiation [27–29], and tissue remodeling in the host [30].

4.3. Mechanical/biological characterization

4.3.1. Biological characterization

We observed maintenance of structural proteins (laminin, elastin, fibronectin) after decellularization. In particular, the amount of sGAGs was similar before and after decellularization in our model, although their distribution could not be specified in the submucosa of the DM. Glycosaminoglycans are long-chain linear saccharide polymers and major components of ECM that play an important role in the mechanical strength of the tissue and in attracting calcium ions owing to their high negative charge. Their absence may favor the appearance of calcium phosphate because of their high negative charge [31]. Thus, the importance of sGAGs preservation has been emphasized, particularly in a porcine aortic DM model [32].

4.3.1.1. Mechanical characterization. Our results are not comparable to those of Badylak et al. [33] for two main reasons: their matrix consisted in a porcine bladder in a canine model and the tensile tests were performed on rectangular samples. The originality of our tests was based on traction of the complete tubular structure as opposed to a planar sample. In longitudinal traction our DMs exhibited higher stresses associated with an increase in elasticity modulus. These characteristics were not found in circumferential traction where a reverse trend was observed: since DM is more prone to deformation and less rigid than NE, it may facilitate food bolus transit through the DM tube since neither innervation, nor musculature is present immediately after grafting. On the other hand, if the DM is too deformable, a bezoar may form. Our burst tests are close to those of Bhrany et al. [16] who tested a decellularized esophageal matrix in a murine model. However, we observed higher intraluminal constraints for DM (108 kPa versus 79.2 kPa, $p = 0.363$). This superiority was also observed in

Table 3
Postoperative complications in six pigs after esophagectomy and decellularized matrix (DM) substitution.

Post-operative complications			DM with maturation in omentum			DM without maturation in omentum		
			Specimens					
			1	2	3	4	5	6
Postoperative mortality			No	Yes	No	No	No	No
Postoperative morbidity	Clinical events	Sialorrhea	Yes	–	Yes	No	No	No
		Vomiting	No	–	No	No	No	No
		Weight loss (%)	26	–	26	17	7	11
	Pathologies observed at explantation	Fistula	Yes	–	No	Yes	No	No
		Abscess	Yes	–	Yes	Yes	No	No
		Stenosis	No	–	Yes	No	No	Yes
		Dilatation	No	–	Yes	No	No	Yes
		Pulmonary infection	No	–	No	Yes	No	No

longitudinal traction. Indeed, our DMs supported higher stresses and tensile forces than NE. These results confirm that the mechanical properties of the esophagus are fulfilled by ECM. Collagen and elastin have a central role in the mechanical function of the esophagus [34]. The helical organization of the collagen fibers in the mucosa confers its anisotropic characteristics, whereas the orthogonal organization of the muscle fibers gives the muscularis its orthotropic character [35]. Yang et al. [2006] tested the mechanical characteristics in porcine esophagus [36]. Their specimens were rectangular and the tests were carried out on the mucosa and the muscularis separately. The mucosal and muscular stresses in longitudinal traction were 9.4 MPa and 1.5 MPa respectively, while in circumferential tension, the mucosal and muscular stresses were 5.3 MPa and 1.2 MPa in that study [36]. These discrepancies with our values can be explained by the esophagus sampling (full thickness tubular shape in our case). Finally, the number of samples tested was insufficient in our study to draw statistically reliable conclusions ($n < 30$). This insufficient number is explained by the desire to perform mechanical tests on the esophagus in its original form and not on two-dimensional (rectangular) samples. Dividing each esophagus into several parts would have allowed multiplying the number of tests but would not have been representative of the mechanical behavior *in situ*. However, we observed similar mechanical behavior with greater stresses in longitudinal traction and similar percentages of deformation. These properties were maintained after decellularization in our study. The values of mechanical parameters of swine esophagus differ from those of its human counterpart [37]. The latter study performed longitudinal and circumferential tensile measurements on human esophagi harvested from fresh cadavers and the longitudinal and circumferential tensile stresses were estimated at 1.67 MPa and 1.48 MPa, respectively [37]. Our circumferential tension results (0.146 MPa), i.e., lower than those obtained with human esophagi [37]. However, the mechanical behavior of the porcine esophagus also differs from its human counterpart, which renders the comparison of DM to human esophagus extraneous.

With these encouraging results we decided to go one step further and test the *in vivo* implantation in a porcine model, after having assessed the biocompatibility of our DM model.

4.4. Biocompatibility

4.4.1. In vitro biocompatibility

DMs are non-cytotoxic in MTT and NR *in vitro* tests according to the ISO 10993 standard. The impregnation of matrices by culture medium molecules (growth factors in fetal calf serum and nutrients) in the last decellularization wash could promote ADSCs' adhesion and survival.

4.4.1.1. In vivo biocompatibility. The use of a histomorphologic score [38,39] enabled the evaluation of tissue integration quality. This was performed at 14 and 35 days after DM implantation in rat muscle wall. Results showed good DM biocompatibility (score > 10) at D14 but not at D35 (score = 8). Since this histomorphologic scoring method is semi-quantitative, it could only give an approximation of biomaterial integration. Keane et al. coupled this assay to the quantification of M1 and M2 macrophages [30]. The M1 phenotype was identified by the presence of $CD68^{+}CD86^{+}$ markers (M1 phenotype) and the M2 phenotype by $CD68^{+}CD206^{+}$ (M2 phenotype) markers. The M2/M1 ratio evaluated the extent of inflammation; the higher the ratio, the better the tissue integration. These two tests applied together permit a better assessment of biological integration. We did not have the technical means to carry out the quantification and the automated calculation of the macrophage ratio.

4.5. Cellularization

The choice of the DM re-cellularization before implantation was based on prior scientific findings, such as the reduction of post-implantation fibrosis and better tissue regeneration of implanted DM [8,10]. The choice of cell type was relatively narrow, and was oriented towards (i) one or more differentiated cell types, or (ii) a stem cell type. Since the majority of esophageal replacements are needed in cases of oncological esophageal ablation, harvesting autologous epithelial or muscle cells of gastrointestinal origin may potentially be amenable to criticism. Also, the stem cells' potential to transform into various lineages made the choice of the latter more appropriate. Among stem cells, the choice between adult embryonic stem cells and induced pluripotent stem cells (IPS) was in favor of the former because those offered the ethical advantage of withdrawal and the practical benefit of availability in large quantities. The technical ease of sampling - a minimally invasive surgical procedure - was also an important criterion. The adipose tissue-derived stem cells (ADSCs) met all of these expectations. ADSCs and SVFs are two distinct but closely related entities in regenerative medicine [40]. The SVF is a mesenchymal cell population comprising four different cell types identified by their surface cell markers analyzed in flow cytometry [41]. Li et al. quantified cell subsets of the SVF and determined that ADSCs accounted for $67.6 \pm 29.7\%$ of cells [42]. Stilleart et al. were the first to observe that the use of SVF in tissue engineering in a murine model induced angiogenesis secondary to the secretion of angiogenic factors [43]. ADSCs secrete a wide variety of growth and angiogenic factors (e.g., vascular endothelial growth factor) favoring angiogenesis in an ischemic medium [44], play an immune role, and are already used in clinical practice especially in plastic and reconstructive surgery [45]. Clinical trials of ADSCs are underway in gastrointestinal surgery (treatment of fistulas in Crohn's disease) [46] and their use would be possible in near future in cardiology, hepatology, and orthopedics [40]. Therefore, ADSCs transpire as the stem cells of choice for cellularizing an esophageal DM. Their isolation, characterization, and culture have been already largely controlled in laboratory, as it was confirmed in the present study with regards to the characterization of the hADSCs we extracted.

4.5.1. Internal/external seeding with hADSC sheets

Regarding the DM's seeding with hADSC sheets, we obtained unsatisfactory cellularization on the luminal surface, whereas cell adhesion and migration did occurs from the DM's external surface. Primary adhesion of the sheet to DM transpired as an important factor in cell migration. The esophageal mucosa, however, constitutes a barrier just as other epithelia in the body. This role of barrier is fulfilled in a state of global equilibrium (cell renewal, submucosal gland secretion, peristalsis), which we aimed to break through decellularization. On the mucosal side ADSCs did not migrate from the lumen, yet adhesion to the underlying submucosa occurred through fissures in the mucosa. The encouraging element is that the concept of cellularization by sheets is viable. The optimal time to culture the sheet with the DM remains to be determined, and so do the culture conditions (dynamic or static).

4.5.1.1. Intraluminar seeding with pADSC and pSVF. On the other hand, DMs were seeded after removal of their mucous membrane by pADSCs or pSVF directly from the lumen. The chosen incubation times were 4 h and 24 h, the aim being to find an incubation time long enough to allow the cells to adhere, but still sufficiently short to avoid excessive manipulations that might lead to contamination (culture media changes), and to allow better cell survival. DMs seeded with pADSCs showed after 24 h organized and elongated cells aligned along and within the submucosa. The DMs seeded

with pSVFs showed many isolated or clumps of round cells inside the submucosa, and sometimes even reaching the border of the muscularis (data not shown). Since these cells were just extracted and had not been grown, they did not show any specific organization between them, and therefore, penetrated deeper into the DM. In addition to pADSCs, pSVF also contains many elements derived from extraction and other cell types such as endothelial progenitors. This molecular and cellular mix may play a role in the migration and survival of pSVF cells and act in cell proliferation and differentiation *in situ*. The pADSCs were isolated from the pSVF by culturing. During this phase, the pADSCs divided and organized on the culture flask. This phase of cultivation seemed to allow them better organization within the DM, but limited their migratory capacity. These results show that it is possible to cellularize DM by this technique in a relatively short time and by greatly limited manipulations. However, new tests should be carried out for further data and to increase the reproducibility and homogeneity of this seeding technique. Nonetheless, cell survival and proliferative capacity within the DM should be studied to check the viability of the injected cells and verify their survival capacity within the DM. The number of cells to be seeded may also have to be adjusted as a function of cell survival *in situ* and relevant biological and clinical impact.

Differentiation of stem cells within matrices has not been clearly demonstrated in all types of DM [47] and their effect could also be paracrine in nature [48,49]. The power of ADSCs on the microenvironment could have an accessory action to their own differentiation once in a biological matrix [47]. The use of autologous stem cells such as ADSCs has raised the problem of these cells' potential carcinogenesis because they chiefly originate from cancer patients [40]. The use of ADSCs in such clinical conditions has already been the subject of clinical studies and has shown encouraging results [50]. ADSCs, however, appear to stimulate tumor cell multiplication by inhibiting cell death under *in vivo* conditions [51]. The exact mechanisms of the effect of autologous ADSCs on patients with progressive cancer are unknown. Their use in the surgical/oncological clinical practice should be cautious and controlled, yet short of absolutely contra-indicating it since their potential mischief is currently not scientifically proven [40].

4.5.1.2. In vivo omentum maturation. Another way to cellularize DM in this study was by means of maturation in omentum. The use of this technique has hitherto been based on empirical clinical conviction short of scientific evidence [52–56]. The use of the omentum in gastrointestinal surgery is commonplace and learning to master it is part of the syllabus in surgical training. In order to evaluate the potential benefit of DM implantation in omentum we performed a preclinical study on a murine model (nude rat). This choice was based on the need to use a mammal (because all have a large omentum [52]. Such an experiment aiming to evaluate the effect over different periods of time of DMs of porcine origin populated with human ADSCs and implanted in rodents, necessitated the use of innate immunotolerant nude rats as hosts, because these can accept MHC-mismatched organ allografts or xenografts for several months. The results established the benefit of such a strategy at the tissue level without major clinical drawbacks. All rats survived and their weight curves appeared normal. These preclinical data permitted assessing the procedure's feasibility under clinical conditions. We have demonstrated the presence of cells in the DM's submucosa - a cellular infiltrate consisting mainly of inflammatory and fibroblastic cells. These data were necessary to confirm the feasibility of DM recellularization. Additionally, the presence of blood capillaries in DMs, even in the submucosal layers, elicits to some extent the consideration of a solution to the vascularization of DMs. The vascularization of matrices is necessary to ensure the transport of oxygen and nutrients within them [57] in order to enable stimulating cell migration within the biomaterial, yet this challenge proved a gridlock in tissue engineering [57,58]. Finally, the use of omentum has knocked down the technological barrier to vascularization. The main obstacle to this method has been the almost complete lack of regulation over omental maturation. However, maturation is controlable by way of the omental implantation duration and the prior addition of cells to the DM. The optimal latency required for DM maturation remains to be determined. There has been a broad literature on the subject, namely, implantation times range from 1 to 12 weeks [59,60]. At 2 weeks of maturation a severe inflammatory reaction was marked by a peak infiltrate suggesting that this interval was too short. However, it was interesting to note that DM vascularization was already present after only 2 weeks of maturation in our study, as well as in another recent work [20]. At 4 weeks vascularization persisted but with a regression in the cellular inflammatory infiltrate. Cells were present even in the DM's submucosa. The DMs showed signs of degradation but their architecture was preserved. After 8 weeks of maturation, more than half of DMs have disappeared, confirming their degradable nature but also that this interval was too long. Consequently, the 4-week delay was deemed the optimal DM maturation period in our study.

Seeding DMs with hADSCs before implantation altered cellular infiltration. DM vascularization was unchanged, without evidence of benefit or drawback on histological analysis. At 4 weeks of maturation, the cellular infiltrate was present even in the submucosa without change in the quantity or quality of the infiltrate. The real benefit of DM's cell seeding before maturation is clearly not demonstrated in our study despite findings to contrary in the literature [10,20,61]. The hypotheses explaining the absence of benefit would lie in the cellularization method, cell type, and animal model. Even though the method of cellularization has shown encouraging *in vitro* results, its potential re-evaluation should not be excluded. The cell type (ADSC) is not questioned, yet its source might be objectionable. Indeed, the source of ADSC sampling should be porcine and autologous. This would entail switching to another animal model. Ideally, in order to formulate more reliable conclusions, pADSCs should be grown in sheet form, placed on the DM that is, in turn, implanted in the greater omentum of a swine; under such conditions, the potential conclusions could be more pertinent, without however being necessarily extrapolatable to humans. Given the encouraging results obtained by Catry et al., another option would be to reproduce our method of seeding DMs with mesenchymal stem cells (MSCs) [20].

The large omentum remains a good bioreactor on account of its easy accessibility by surgical techniques that have become clinical routine and its demonstrated intrinsic qualities [53–56] sanctioning its use in regenerative medicine.

4.6. DM implantation in a pig model

DM implantation after esophagectomy was the ultimate goal of the present study. Currently there is no surgical procedure to replace short esophageal segments without the challenging procedures of gastric pull-up or colon interposition. Keeping some animals alive with an artificial esophagus is a promising result. The first step was to evaluate whether such an intervention was feasible by laparotomy. The choice of excising the lower third of esophagus was motivated by the clinical reality of higher incidence of esophageal adenocarcinomas occurring in the lower third. The transcervical replacement in swine would have been simpler in all aspects (technique, follow-up) but would not have responded to the clinical need. The transabdominal surgical approach has not been hitherto published in animal models. Its surgical feasibility

seemed good. The depth of field (esophageal hiatus) is lesser in pig versus man, making the accessibility of the abdominal and thoracic esophageal segments easy via laparotomy. However, the anatomical associations between the esophagus and pleura appear nearer, especially on the left side, consequently resulting in frequent left-sided intraoperative pneumothorax. The suturability of DM was very good based on the surgeon's assessment (albeit not objectively studied); the PDS 4/0 suture did not cut through the DMs, which indicated good fixedness of the material. We chose a preclinical model close to human [10]. The pig esophagus has morphological characteristics (weight, length, and thickness) similar to the human, which may allow potential transfer to the clinic by designing DMs from either human organ donation or porcine esophagus.

The group of 3 pigs receiving DM after prior maturation in their own omentum permitted to estimate the clinical impact of a second laparotomy, however minor. Indeed, the weight curve of those three animals shifted trajectory. However, the group of six pigs was homogeneous age-wise and we found a difference in body weight at the time of esophageal replacement with an advantage for the group without prior maturation. These findings call for caution as to the safety of an *in vivo* maturation phase. Moreover, this 4-week maturation phase significantly modified the elasticity of DM. The matured DMs were more fibrous, adding a technical constraint during esophageal replacement surgery. Indeed, the caliber incongruence between NE and DM was easily corrected without maturation but it proved more difficult after maturation on account of the matured DM's fibrous nature. There was no technical problem even 4 weeks after a first laparotomy. The vascularization of the DM through the omentum was macroscopically visible and the latter's surgical non-violation proved undemanding. The resumption of feeding on a hypercaloric liquid fraction was authorized on the evening of intervention and continued throughout the first week without quantity restriction. This postoperative strategy of “early rehabilitation” enabled dispensing with enteral or parenteral nutritional support. The early rehabilitation strategy is currently being studied in esogastric surgery [62] but has already demonstrated its effectiveness in other surgical specialties [63]. An individual had fever and died on the first post-operative day. Autopsy extracted an intraperitoneal abdominal mesh located in the left hypochondrium and the death was attributed to this “textiloma” for lack of another plausible explanation. Only one individual had no postoperative complications, whereas 2 pigs had fistula, 3 had abscess, and 2 had stenosis. Clinical findings were mixed. Nevertheless, the only individual with no complications had a maximum observed weight loss of only 7%. Histological analysis of the implanted DM systematically objectified its tissue regeneration very close to the condition of NE in all individuals. It may be assumed that the anatomical location of the esophagus conditioned its structure and, consequently, its regeneration. On the other hand, the areas affected by fistulas and abscesses showed very significant inflammatory and fibrous changes, which precludes definite conclusions. The absence of a sham group precluded the evaluation of non-specific surgical morbidity caused by laparotomy or anastomoses independently of those imparted by the DM *per se.*

4.7. Our model through the lens of previous attempts

Scrutiny of the literature on recently tested models distinguishes between different approaches in terms of graft characterization and/or animal model, regardless of the method to obtain the tubular tissue to be grafted.

For reasons of graft size and surgery feasibility, the rabbit is often selected because it is larger than rodents: (i) Tessier et al. tested fascial flap-wrapped allogenic aorta (AA) segments with disappointing clinical results despite finding incipient remodeling of the esophageal substitute [64], (ii) Park et al. evaluated a 3-D-printed cellularized patch of polycaprolactone as cervical esophagus substitute with successful results in terms of remodeling and clinical outcomes [65], and (iii) Maughan et al. implanted a tracheal scaffold for pediatric purposes [66]. On the other hand, Barron et al. [2016] used a pig model to test a 5-cm long polyurethane mucosal non-autologous cell-seeded circumferential graft implanted via thoracotomy and supported by a stent to ensure permanent patency of the structure [67]. Significant remodeling of the graft occurred during the animal's 29-day follow-up but this encouraging single test is insufficient to conclude. The approach chosen by Catry et al. was closest to ours, by having tested a cellularized porcine small intestinal submucosa (SIS) seeded with MSCs and matured for 14 days in porcine omentum [20]. However, their interesting results in terms of recellularization were impaired by the heterogeneity of animals' survival closely linked to frequent and repeated stent migration and subsequent stricture. Using a stent has severe drawbacks that surgeons would like to avoid [68] even though no alternative exists as of yet.

Interestingly, Den Hondt et al. chose a method very similar to ours to evaluate a decellularized rabbit trachea in terms of decellularization process, biological, and mechanical characterization of the substitute, yet for the latter they developed an ingenious microCT analysis that was non-destructive of the construct [69].

4.8. Limits of the model and perspectives

We demonstrated the ability to produce a 5-cm-long tubular tissue-engineered esophageal graft and evaluate its integration in a pig model of esophagectomy. For this purpose, we chose to decellularize a pig esophagus. Criteria of effective decellularization are not consensual. Crapo et al. [25] described simple criteria to assess effective decellularization, i.e.: (i) no intact nuclei visible with histologic staining or DAPI, (ii) quantity of residual DNA < 50 ng/mg weight dry tissue, and (iii) length of residual DNA > 200 bp. The decellularization method is different for each specific tissue but generally includes applying reagents (such as detergents and enzymes) and/or physical methods [25]. Our decellularization process of pig esophagi proved efficient in terms of the Crapo et al. criteria [25]. It was also reproducible and led to a biocompatible matrix that was amenable to cellularization and proved implantable. It is not mandatory to look for a longer and/or innervated circumferential graft since the replacement of a short segment can be sufficient to save the whole organ. In this case, the absence of innervation and motility is, although not satisfactory, less crucial. However, regarding the prospect of clinical translation of this concept, the preservation conditions of the DM are a challenging issue. Cryopreservation proposed by Urbani et al. [70] seems to be promising and should be tested in our model. Then, biocompatibility and mechanical tests should be redone to assess the suitability of this technique to our DM. The cellularization, or in other words “revitalization”, of the matrix before implantation cannot be avoided in order to ensure the proper integration of the esophageal substitute and reduce the risk of fistula. However, this implies following up the cells and assess their viability and behavior after transplantation.

Our animal model of choice had pros and cons: (i) we avoided the thoracotomy approach to facilitate animal follow-up although this is not the most prevalent choice transpiring from the literature [67]; (ii) we preserved the esophagogastric junction to avoid the natural heavy reflux although 90% of the target population undergo the resection of this area; iii) one may assume that the model is functional because of our DM's high burst pressure (no blow-out by food transit is feared) and because the animals gained weight; (iv) we should further investigate the impact on esophageal physiology

by a manometry study and lengthen the animals' follow up; (v) the formation of fistulas within anastomoses during the early phase remains the main issue to be addressed, by means of DM cellularization, or by using autologous platelet-rich plasma spraying [68], in order to improve healing kinetics.

5. Conclusion

We set up a biological tissue-engineered biocompatible esophageal graft made of DM and protein with architectural properties similar to the native porcine esophagus. Its lack of cytotoxicity allowed seeding with adult mesenchymal stem cells. The clinical applications of this study may concern reconstructions after ablation of esophago-tracheal fistulas, small adenocarcinomas of the lower third of the esophagus, and potentially providing a solution to long-gap esophageal atresia [71]. This work will widen the knowledge on the pros and cons of the potential use of decellularized tissues as organ substitutes.

Funding

This work was supported by Fondation de l'Avenir in 2013 (ET3-699) and 2015 (AP-RMA-2015-005), and Fédération de Recherche TecSan of Bordeaux University in 2015.

Acknowledgments

We thank Sandro Cornet, Martine Renard, Fanny Blaudez, Clémence Lewden of CIC1401 (Bordeaux University Hospital, France) for burst pressure tests, assistance in cytotoxicity studies and support in pidg implantation; Jérôme Kalisky, Robin Siadous, Damien Le Nihouannen (U1026 BIOTIS Inserm, Bordeaux University, France) for DM sterilization, assistance in DNA isolation and quantification, SEM analysis and flow cytometry assistance; S. Ferchaud of INRA for pig implantation supervision; Lucy Germain (LOEX, Québec, Canada) for her advice on cell sheet culture; DETERCA (Bordeaux University, France) and IHU LIRYC (Bordeaux University, France) for providing pigs from previous experiments and access to their facilities for esophagi's harvesting; RESCOLL (Pessac, France) for performing traction testing on DM.

Appendix A. Supplementary data

Supplementary data related to this article can be found at https://doi.org/10.1016/j.biomaterials.2018.05.023.

References

[1] J.B. Hulscher, J.W. van Sandick, A.G. de Boer, B.P. Wijnhoven, J.G. Tijssen, P. Fockens, et al., Extended transthoracic resection compared with limited transhiatal resection for adenocarcinoma of the esophagus, N. Engl. J. Med. 347 (2002) 1662–1669, https://doi.org/10.1056/NEJMoa022343.
[2] A. Sauvanet, C. Mariette, P. Thomas, P. Lozac'h, P. Segol, E. Tiret, et al., Mortality and morbidity after resection for adenocarcinoma of the gastroesophageal junction: predictive factors, J. Am. Coll. Surg. 201 (2005) 253–262, https://doi.org/10.1016/j.jamcollsurg.2005.02.002.
[3] S.G. Swisher, L. Deford, K.W. Merriman, G.L. Walsh, R. Smythe, A. Vaporicyan, et al., Effect of operative volume on morbidity, mortality, and hospital use after esophagectomy for cancer, J. Thorac. Cardiovasc. Surg. 119 (2000) 1126–1132, https://doi.org/10.1067/mtc.2000.105644.
[4] N. Briez, G. Piessen, F. Torres, G. Lebuffe, J.P. Triboulet, C. Mariette, Effects of hybrid minimally invasive esophagectomy on major postoperative pulmonary complications, Br. J. Surg. 99 (2012) 1547–1553, https://doi.org/10.1002/bjs.8931.
[5] S.S. Biere, M.I. van Berge Henegouwen, K.W. Maas, L. Bonavina, C. Rosman, J.R. Garcia, et al., Minimally invasive versus open oesophagectomy for patients with oesophageal cancer: a multicentre, open-label, randomised controlled trial, Lancet 379 (2012) 1887–1892, https://doi.org/10.1016/S0140-6736(12)60516-9.
[6] A.D. Bhrany, C.J. Lien, B.L. Beckstead, N.D. Futran, N.H. Muni, C.M. Giachelli, B.D. Ratner, Crosslinking of an oesophagus acellular matrix tissue scaffold, J Tissue Eng Regen Med 2 (2008) 365–372, https://doi.org/10.1002/term.105.
[7] P.Y. Chu, S.Y. Chang, Reconstruction of the hypopharynx after surgical treatment of squamous cell carcinoma, J. Chin. Med. Assoc. 72 (2009) 351–355, https://doi.org/10.1016/S1726-4901(09)70386-7.
[8] J.Y. Tan, C.K. Chua, K.F. Leong, K.S. Chian, W.S. Leong, L.P. Tan, Esophageal tissue engineering: an in-depth review on scaffold design, Biotechnol. Bioeng. 109 (2012) 1–15, https://doi.org/10.1002/bit.23323.
[9] P. Kuppan, S. Sethuraman, U.M. Krishnan, Tissue engineering interventions for esophageal disorders – promises and challenges, Biotechnol. Adv. 30 (2012) 1481–1492, https://doi.org/10.1016/j.biotechadv.2012.03.005.
[10] G. Luc, M. Durand, D. Collet, F. Guillemot, L. Bordenave, Esophageal tissue engineering, Expet Rev. Med. Dev. 11 (2014) 225–241, https://doi.org/10.1586/17434440.2014.870470.
[11] K.H. Song, New techniques for treating an anal fistula, J Korean Soc Coloproctol 28 (2012) 7–12, https://doi.org/10.3393/jksc.2012.28.1.7.
[12] H.C. Ott, B. Clippinger, C. Conrad, C. Schuetz, I. Pomerantseva, L. Ikonomou, et al., Regeneration and orthotopic transplantation of a bioartificial lung, Nat. Med. 16 (2010) 927–933, https://doi.org/10.1038/nm.2193.
[13] R. Langer, D.A. Tirrell, Designing materials for biology and medicine, Nature 428 (2004) 487–492, https://doi.org/10.1038/nature02388.
[14] P. Bornstein, E.H. Sage, Matricellular proteins: extracellular modulators of cell function, Curr. Opin. Cell Biol. 14 (2002) 608–616.
[15] J.A. Hawkins, N.D. Hillman, L.M. Lambert, J. Jones, G.B. Di Russo, T. Profaizer, et al., Immunogenicity of decellularized cryopreserved allografts in pediatric cardiac surgery: comparison with standard cryopreserved allografts, J. Thorac. Cardiovasc. Surg. 126 (2003) 247–252 discussion 252–253.
[16] A.D. Bhrany, B.L. Beckstead, T.C. Lang, D.G. Farwell, C.M. Giachelli, B.D. Ratner, Development of an esophagus acellular matrix tissue scaffold, Tissue Eng. 12 (2006), https://doi.org/10.1089/ten.2006.12.319, 319 → 30.
[17] B.L. Beckstead, S. Pan, A.D. Bhrany, A.M. Bratt-Leal, B.D. Ratner, C.M. Giachelli, Esophageal epithelial cell interaction with synthetic and natural scaffolds for tissue engineering, Biomaterials 26 (2005) 6217–6228, https://doi.org/10.1016/j.biomaterials.2005.04.010.
[18] S. Badylak, S. Meurling, M. Chen, A. Spievack, A. Simmons-Byrd, Resorbable bioscaffold for esophageal repair in a dog model, J. Pediatr. Surg. 35 (2000) 1097–1103, https://doi.org/10.1053/jpsu.2000.7834.
[19] M.F. Lopes, A. Cabrita, J. Ilharco, P. Pessa, J. Patrício, Grafts of porcine intestinal submucosa for repair of cervical and abdominal esophageal defects in the rat, J. Invest. Surg. 19 (2006) 105–111, https://doi.org/10.1080/08941930600569621.
[20] J. Catry, M. Luong-Nguyen, L. Arakelian, T. Poghosyan, P. Bruneval, T. Domet, et al., Circumferential esophageal replacement by a tissue-engineered substitute using mesenchymal stem cells: an experimental study in mini pigs, Cell Transplant. 26 (2017) 1831–1839, https://doi.org/10.1177/0963689717741498.
[21] J.A. Isch, S.A. Engum, C.A. Ruble, M.M. Davis, J.L. Grosfeld, Patch esophagoplasty using AlloDerm as a tissue scaffold, J. Pediatr. Surg. 36 (2001) 266–268, https://doi.org/10.1053/jpsu.2001.20685.
[22] B.A. Bunnell, M. Flaat, C. Gagliardi, B. Patel, C. Ripoll, Adipose-derived stem cells: isolation, expansion and differentiation, Methods 45 (2008) 115–120, https://doi.org/10.1016/j.ymeth.2008.03.006.
[23] T. Mosmann, Rapid colorimetric assay for cellular growth and survival: application to proliferation and cytotoxicity assays, J. Immunol. Meth. 65 (1983) 55–63.
[24] E. Borenfreund, J.A. Puerner, Toxicity determined in vitro by morphological alterations and neutral red absorption, Toxicol. Lett. 24 (1985) 119–124.
[25] P.M. Crapo, T.W. Gilbert, S.F. Badylak, An overview of tissue and whole organ decellularization processes, Biomaterials 32 (2011) 3233–3243, https://doi.org/10.1016/j.biomaterials.2011.01.057.
[26] E. Vorotnikova, D. McIntosh, A. Dewilde, J. Zhang, J.E. Reing, L. Zhang, Extracellular matrix-derived products modulate endothelial and progenitor cell migration and proliferation in vitro and stimulate regenerative healing in vivo, Matrix Biol. 29 (2010) 690–700, https://doi.org/10.1016/j.matbio.2010.08.007.
[27] J.L. Xu, K.A. Khor, Y.W. Lu, W.N. Chen, R. Kumar, Osteoblast interactions with various hydroxyapatite based biomaterials consolidated using a spark plasma sintering technique, J. Biomed. Mater. Res. B Appl. Biomater. 84 (2008) 224–230, https://doi.org/10.1002/jbm.b.30864.
[28] A. Parekh, B. Mantle, J. Banks, J.D. Swarts, S.F. Badylak, J.E. Dohar, P.A. Hebda, Repair of the tympanic membrane with urinary bladder matrix, Laryngoscope 119 (2009) 1206–1213, https://doi.org/10.1002/lary.20233.
[29] J.E. Valentin, D.O. Freytes, J.M. Grasman, C. Pesyna, J. Freund, T.W. Gilbert, S.F. Badylak, Oxygen diffusivity of biologic and synthetic scaffold materials for tissue engineering, J. Biomed. Mater. Res. 91 (2009) 1010–1017, https://doi.org/10.1002/jbm.a.32328.
[30] T.J. Keane, I.T. Swinehart, S.F. Badylak, Methods of tissue decellularization used for preparation of biologic scaffolds and in vivo relevance, Methods 84 (2015) 25–34, https://doi.org/10.1016/j.ymeth.2015.03.005.
[31] N. Vyavahare, M. Ogle, F.J. Schoen, R. Zand, D.C. Gloeckner, M. Sacks, R.J. Levy, Mechanisms of bioprosthetic heart valve failure: fatigue causes collagen denaturation and glycosaminoglycan loss, J. Biomed. Mater. Res. 46 (1999) 44–50.
[32] B. Mendoza-Novelo, E.E. Avila, J.V. Cauich-Rodríguez, E. Jorge-Herrero, F.J. Rojo, G.V. Guinea, J.L. Mata-Mata, Decellularization of pericardial tissue

and its impact on tensile viscoelasticity and glycosaminoglycan content, Acta Biomater. 7 (2011) 1241–1248, https://doi.org/10.1016/j.actbio.2010.11.017.
[33] S.F. Badylak, D.A. Vorp, A.R. Spievack, A. Simmons-Byrd, J. Hanke, D.O. Freytes, et al., Esophageal reconstruction with ECM and muscle tissue in a dog model, J. Surg. Res. 128 (2005) 87–97, https://doi.org/10.1016/j.jss.2005.03.002.
[34] E.A. Stavropoulou, Y.F. Dafalias, D.P. Sokolis, Biomechanical and histological characteristics of passive esophagus: experimental investigation and comparative constitutive modeling, J. Biomech. 42 (2009) 2654–2663, https://doi.org/10.1016/j.jbiomech.2009.08.018.
[35] A.N. Natali, E.L. Carniel, H. Gregersen, Biomechanical behavior of oesophageal tissues: material and structural configuration, experimental data and constitutive analysis, Med. Eng. Phys. 31 (2009) 1056–1062, https://doi.org/10.1016/j.medengphy.2009.07.003.
[36] W. Yang, T.C. Fung, K.S. Chian, C.K. Chong, Directional, regional, and layer variations of mechanical properties of esophageal tissue and its interpretation using a structure-based constitutive model, J. Biomech. Eng. 128 (2006) 409–418, https://doi.org/10.1115/1.2187033.
[37] I. Vanags, A. Petersons, V. Ose, I. Ozolanta, V. Kasyanov, J. Laizans, Biomechanical properties of oesophagus wall under loading, J. Biomech. 26 (2003) 1387–1390.
[38] B.N. Brown, R. Londono, S. Tottey, L. Zhang, K.A. Kukla, M.T. Wolf, et al., Macrophage phenotype as a predictor of constructive remodeling following the implantation of biologically derived surgical mesh materials, Acta Biomater. 8 (2012) 978–987, https://doi.org/10.1016/j.actbio.2011.11.031.
[39] T.J. Keane, R. Londono, R.M. Carey, C.A. Carruthers, J.E. Reing, C.L. Dearth, et al., Preparation and characterization of a biologic scaffold from esophageal mucosa, Biomaterials 34 (2013) 6729–6737, https://doi.org/10.1016/j.biomaterials.2013.05.052.
[40] S.S. Tan, W. Loh, The utility of adipose-derived stem cells and stromal vascular fraction for oncologic soft tissue reconstruction: is it safe? A matter for debate, Surgeon 15 (2017) 186–189, https://doi.org/10.1016/j.surge.2016.09.010.
[41] K. Doi, S. Tanaka, H. Iida, H. Eto, H. Kato, N. Aoi, et al., Stromal vascular fraction isolated from lipo-aspirates using an automated processing system: bench and bed analysis, J Tissue Eng Regen Med 7 (2013) 864–870, https://doi.org/10.1002/term.1478.
[42] H. Li, L. Zimmerlin, K.G. Marra, V.S. Donnenberg, A.D. Donnenberg, J.P. Rubin, Adipogenic potential of adipose stem cell subpopulations, Plast. Reconstr. Surg. 128 (2011) 663–672, https://doi.org/10.1097/PRS.0b013e318221db33.
[43] F. Stillaert, M. Findlay, J. Palmer, R. Idrizi, S. Cheang, A. Messina, et al., Host rather than graft origin of Matrigel-induced adipose tissue in the murine tissue-engineering chamber, Tissue Eng. 13 (2007) 2291–2300.
[44] S.T. Hsiao, A. Asgari, Z. Lokmic, R. Sinclair, G.J. Dusting, S.Y. Lim, R.J. Dilley, Comparative analysis of paracrine factor expression in human adult mesenchymal stem cells derived from bone marrow, adipose, and dermal tissue, Stem Cell. Dev. 21 (2012) 2189–2203, https://doi.org/10.1089/scd.2011.0674.
[45] S.F. Kølle, A. Fischer-Nielsen, A.B. Mathiasen, J.J. Elberg, R.S. Oliveri, P.V. Glovinski, et al., Enrichment of autologous fat grafts with ex-vivo expanded adipose tissue-derived stem cells for graft survival: a randomized placebo-controlled trial, Lancet 382 (2013) 1113–1120, https://doi.org/10.1016/S0140-6736(13)61410-5.
[46] D. Garcia-Olmo, D. Herreros, I. Pascual, J.A. Pascual, E. Del-Valle, J. Zorrilla, et al., Expanded adipose-derived stem cells for the treatment of complex perianal fistula: a phase II clinical trial, Dis. Colon Rectum 52 (2009) 79–86, https://doi.org/10.1007/DCR.0b013e3181973487.
[47] G. Agmon, K.L. Christman, Controlling stem cell behavior with decellularized extracellular matrix scaffolds, Curr. Opin. Solid State Mater. Sci. 20 (2016) 193–201, https://doi.org/10.1016/j.cossms.2016.02.001.
[48] D.M. Hoganson, A.M. Meppelink, C.J. Hinkel, S.M. Goldman, X.H. Liu, R.M. Nunley, et al., Differentiation of human bone marrow mesenchymal stem cells on decellularized extracellular matrix materials, J. Biomed. Mater. Res. 102 (2014) 2875–2883, https://doi.org/10.1002/jbm.a.34941.
[49] R.H. Fu, Y.C. Wang, S.P. Liu, T.R. Shih, H.L. Lin, Y.M. Chen, et al., Decellularization and recellularization technologies in tissue engineering, Cell Transplant. 23 (2014) 621–630, https://doi.org/10.3727/096368914X678382.
[50] R. Pérez-Cano, J.J. Vranckx, J.M. Lasso, C. Calabrese, B. Merck, A.M. Milstein, et al., Prospective trial of adipose-derived regenerative cell (ADRC)-enriched at grafting for partial mastectomy defects: the RESTORE-2 trial, Eur. J. Surg. Oncol. 38 (2012) 382–389, https://doi.org/10.1016/j.ejso.2012.02.178.
[51] J.M. Yu, E.S. Jun, Y.C. Bae, J.S. Jung, Mesenchymal stem cells derived from human adipose tissues favor tumor cell growth in vivo, Stem Cell. Dev. 17 (2008) 463–473, https://doi.org/10.1089/scd.2007.0181.
[52] R. Morison, Remarks on some functions of the omentum, Br. Med. J. 1 (1906) 76–78.
[53] S. Shah, E. Lowery, R.K. Braun, A. Martin, N. Huang, M. Medina, et al., Cellular basis of tissue regeneration by omentum, PLoS One 7 (2012) e38368, https://doi.org/10.1371/journal.pone.0038368.
[54] A.H. Moreschi, A.V. Macedo Neto, G.V. Barbosa, M.G. Saueressig, Aggressive treatment using muscle flaps or omentopexy in infections of the sternum and anterior mediastinum following sternotomy, J. Bras. Pneumol. 34 (2008) 654–660.
[55] C. Vatansev, M.E. Ustün, C.O. Oğün, G. Taştekin, A. Karabacakoğlu, H. Yilmaz, Omental transposition decreases ischemic brain damage examined in a new ischemia model, Eur. Surg. Res. 34 (2003) 388–394, https://doi.org/10.1159/000070612.
[56] C.T. Maloney Jr., D. Wages, J. Upton, W.P. Lee, Free omental tissue transfer for extremity coverage and revascularization, Plast. Reconstr. Surg. 111 (2003) 1899–1904, https://doi.org/10.1097/01.PRS.0000056874.31920.7D.
[57] H.C. Ko, B.K. Milthorpe, C.D. McFarland, Engineering thick tissues—the vascularization problem, Eur. Cell. Mater. 14 (2007) 1–18 discussion 18–19.
[58] L.G. Griffith, G.T. Naughton, Tissue engineering—current challenges and expanding opportunities, Science 295 (2002) 1009–1014, https://doi.org/10.1126/science.1069210.
[59] Y. Takimoto, T. Nakamura, M. Teramachi, T. Kiyotani, Y. Shimizu, Replacement of long segments of the esophagus with a collagen-silicone composite tube, Am. Soc. Artif. Intern. Organs J. 41 (1995) M605–M608.
[60] J.H. Kim, J. Kim, W.H. Kong, S.W. Seo, Factors affecting tissue culture and transplantation using omentum, Am. Soc. Artif. Intern. Organs J. 56 (2010) 349–355, https://doi.org/10.1097/MAT.0b013e3181e4848a.
[61] Y. Nakase, T. Nakamura, S. Kin, S. Nakashima, T. Yoshikawa, Y. Kuriu, et al., Intrathoracic esophageal replacement by in situ tissue-engineered esophagus, J. Thorac. Cardiovasc. Surg. 136 (2008) 850–859, https://doi.org/10.1016/j.jtcvs.2008.05.027.
[62] J.M. Findlay, R.S. Gillies, J. Millo, B. Sgromo, R.E. Marshall, N.D. Maynard, Enhanced recovery for esophagectomy: a systematic review and evidence-based guidelines, Ann. Surg. 259 (2014) 413–431, https://doi.org/10.1097/SLA.0000000000000349.
[63] M.D. Stowers, D.P. Lemanu, A.G. Hill, Health economics in enhanced recovery after surgery programs, Can. J. Anaesth. 62 (2015) 219–230, https://doi.org/10.1007/s12630-014-0272-0.
[64] W. Tessier, C. Mariette, M.C. Copin, W.B. Robb, R. Jashari, T. Hubert, A. Wurtz, Replacement of the esophagus with fascial flap-wrapped allogenic aorta, J. Surg. Res. 193 (2015) 176–183, https://doi.org/10.1016/j.jss.2014.07.033.
[65] S.Y. Park, J.W. Choi, J.K. Park, E.H. Song, S.A. Park, Y.S. Kim, Tissue-engineered artificial oesophagus patch using three-dimensionally printed polycaprolactone with mesenchymal stem cells: a preliminary report, Interact. Cardiovasc. Thorac. Surg. 22 (2016) 712–717, https://doi.org/10.1093/icvts/ivw048.
[66] E.F. Maughan, C.R. Butler, C. Crowley, G.Z. Teoh, M.D. Hondt, N.J. Hamilton, A comparison of tracheal scaffold strategies for pediatric transplantation in a rabbit model, Laryngoscope 127 (2017) E449–E457, https://doi.org/10.1002/lary.26611.
[67] M.R. Barron, E.W. Blanco, J.M. Aho, J. Chakroff, J. Johnson, S.D. Cassivi, Full-thickness oesophageal regeneration in pig using a polyurethane mucosal cell seeded graft, J Tissue Eng Regen Med (2016), https://doi.org/10.1002/term.2386 ([Epub ahead of print]).
[68] K.S. Dua, W.J. Hogan, A.A. Aadam, M. Gasparri, In-vivo oesophageal regeneration in a human being by use of a non-biological scaffold and extracellular matrix, Lancet 388 (2016) 55–61, https://doi.org/10.1016/S0140-6736(15)01036-3.
[69] M. Den Hondt, B.M. Vanaudenaerde, E.F. Maughan, C.R. Butler, C. Crowley, E.K. Verbeken, An optimized non-destructive protocol for testing mechanical properties in decellularized rabbit trachea, Acta Biomater. 60 (2017) 291–301, https://doi.org/10.1016/j.actbio.2017.07.035.
[70] L. Urbani, P. Maghsoudlou, A. Milan, M. Menikou, C.K. Hagen, G. Totonelli, Long-term cryopreservation of decellularized oesophagi for tissue engineering clinical application, PLoS One 12 (2017) e0179341, https://doi.org/10.1371/journal.pone.0179341.
[71] E. Lee, A. Milan, L. Urbani, P. De Coppi, M.W. Lowdell, Decellularized material as scaffolds for tissue engineering studies in long gap esophageal atresia, Expet Opin. Biol. Ther. 17 (2017) 573–584, https://doi.org/10.1080/14712598.2017.1308482.